

# Outward oriented gravitational attraction in the innermost part of the compact objects - a new feature of relativistic gravity

L. Neslušan 

*Astronomical Institute of the Slovak Academy of Sciences  
059 60 Tatranská Lomnica, The Slovak Republic (E-mail: ne@ta3.sk)*

Received: June 27, 2024; Accepted: July 15, 2024

**Abstract.** We point out a new feature of gravity within general relativity (GR): according to GR, the gravity in the innermost region of relativistic compact objects (RCOs) is oriented outward from the object's center. We explain how the normal, attractive, gravity does result in such the orientation. Our analysis of RCO properties, derived from some models which imply the outward oriented action in the RCO central region, indicates that the gaseous RCOs are the objects in the shape of a hollow sphere with an inner physical surface. These inner radii can be arbitrarily small (but it is questionable if ever exactly zero), and this has been, likely, the reason of why the phenomenon of the outward oriented gravity has escaped our attention. We discuss the conceptual differences between the old, fulfilled-sphere, and new, hollow-sphere, concepts of RCO. Until now, the new concept has been forbidden by a postulate, in fact. This prohibition caused that almost whole general relativity was forbidden in the astrophysics of RCOs; the Oppenheimer-Volkoff upper-mass limit is a consequence of this prohibition. In conclusion, we point out that any model of realistic RCOs in the shape of a rigorous fulfilled sphere has never been constructed. It is questionable if such a solution of field equation exists. Within GR, we can easily construct only the models of real stable RCOs in the form of a hollow-sphere.

**Key words:** gravitation – general relativity – neutron stars – supermassive compact objects

## 1. Introduction

In this article, we give a review of gradually improving knowledge about the relativistic compact object (RCO), which should acquire the shape of a hollow-sphere, i.e. the spherical volume constrained not only with an outer, but also an inner physical surface. A large part of this knowledge was published in our previous papers (Neslušan, 2015, 2017a,b, 2019; Neslušan, 2022) and papers by deLyra et al. (deLyra, 2021; deLyra & Carneiro, 2023; deLyra et al., 2023; deLyra, 2023). Anastopoulos & Savvidou (2021) and Kotopoulis & Anastopoulos

(2023) analyzed a thermodynamic consistency of the equation of state, whereby they also dealt with the hollow-sphere solutions. One should, however, be careful with the conclusions drawn in their work since they also considered some unrealistic equations of state and outward oriented gravitational action represented with the help of negative mass. Even before the publishing of all these papers, the first hollow-sphere model of RCO was published by Ni (2011). Our review is completed with some new arguments and explanations.

The new concept of RCO raises a lot of questions. For example, if the RCO in the shape of a hollow sphere is stable; if the metrics inside it and in its vicinity is continuous; why a vacuum void in its central region occurs; what is the mechanism of its formation, etc. Of course, the main question is: how is the hollow-sphere RCO concept related to the currently accepted concept of the RCO in the form of a fulfilled sphere? What are the arguments in favor of each of these two concepts?

A discussion about the new concept is important. The general relativity (GR) provides us with a set of solutions to construct a model of RCO. The extent of this set can be illustrated with an infinite area. In the scheme in Fig. 1, this area is shown with the blue color. The area is bordered, from one side, with an abscissa (drawn with the red color in the scheme). The extent of the solutions implying the RCOs in the form of a fulfilled sphere is proportional only to this abscissa. (At the moment, it is however unknown whether the RCO can acquire the form of an exact or only approximate fulfilled sphere; we discuss this problem in Sect. 4.2.) The area of the one-dimensional abscissa is zero. The scheme in Fig. 1 points out that we are currently allowed to use the zero-area part of the infinite-area set of solutions. Either we should have a very good reason to reject almost all available solutions or we should abolish the prohibition of using them.

## 2. Outline of the theory of RCO

### 2.1. Description of the curvature of space-time

At first, let us outline the theory of RCO in general. In the following, we consider a simple, static, spherically symmetric object. Using the  $---+$  signature and the coordinate system with the spatial part to be the spherical system  $O(r\vartheta\varphi)$ , the line element in the case of spherical symmetry is

$$ds^2 = -e^\lambda dr^2 - r^2 d\vartheta^2 - r^2 \sin^2 \vartheta d\varphi^2 + e^\nu c^2 dt^2, \quad (1)$$

where  $-e^\lambda = g_{11} = g_{rr}$ ,  $-r^2 = g_{22} = g_{\vartheta\vartheta}$ ,  $-r^2 \sin^2 \vartheta = g_{33} = g_{\varphi\varphi}$ , and  $e^\nu = g_{44} = g_{tt}$ . In the static RCO, the auxiliary metric functions  $\lambda$  and  $\nu$  are the functions of only the radial distance,  $r$ .

Since we consider a compact object within GR, gravity must be described by Einstein's field equations (EFEs) (Einstein, 1915, 1916). For the spherically

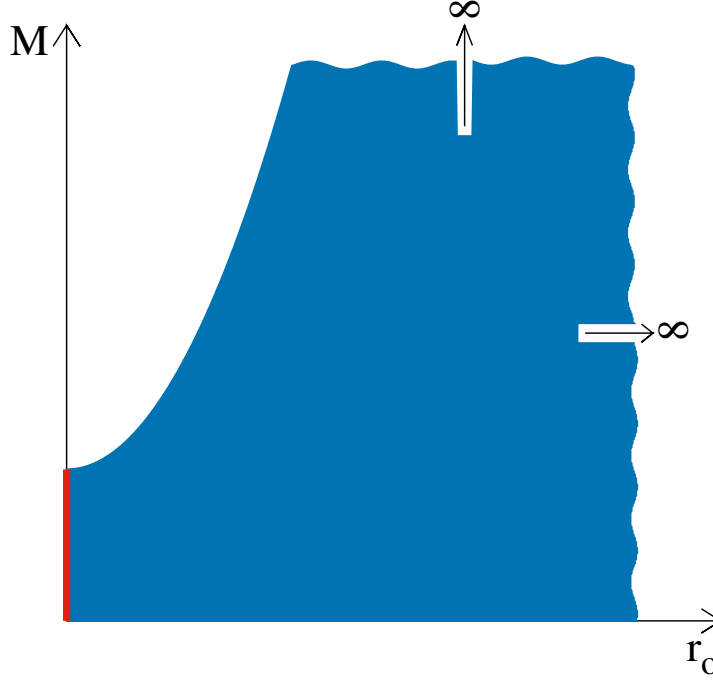


**Figure 1.** The scheme illustrating the whole extent of all GR solutions to describe the RCOs (the blue area continuing to infinity upward and rightward) and extent of the part of solutions which are currently allowed to be used (the red vertical abscissa).

symmetric RCO, these equations acquire the form (Tolman, 1934)

$$\kappa T_1^1 = -e^{-\lambda} \left( \frac{\nu'}{r} + \frac{1}{r^2} \right) + \frac{1}{r^2}, \quad (2)$$

$$\kappa T_2^2 = -e^{-\lambda} \left( \frac{\nu''}{2} - \frac{\lambda' \nu'}{4} + \frac{\nu'^2}{4} + \frac{\nu' - \lambda'}{2r} \right), \quad (3)$$

$$\kappa T_3^3 = -e^{-\lambda} \left( \frac{\nu''}{2} - \frac{\lambda' \nu'}{4} + \frac{\nu'^2}{4} + \frac{\nu' - \lambda'}{2r} \right), \quad (4)$$

$$\kappa T_4^4 = e^{-\lambda} \left( \frac{\lambda'}{r} - \frac{1}{r^2} \right) + \frac{1}{r^2}, \quad (5)$$

$$\kappa T_\mu^\sigma = 0 \quad \text{for } \mu \neq \sigma, \quad (6)$$

where  $\kappa = 8\pi G/c^4$  is the Einstein gravitational constant ( $G$  is the Newton gravitational constant and  $c$  is the speed of light in vacuum) and  $T_\mu^\sigma$  is the stress-energy tensor. The prime indicates the derivative of a given quantity in respect

of  $r$  and the double prime the second derivative in respect of  $r$ . When one deals with the spherically symmetric neutron stars as well as other gaseous spherically symmetric RCOs, the stress-energy tensor for a perfect fluid (Tolman, 1934)

$$T_{\mu}^{\sigma} = \begin{pmatrix} -P & 0 & 0 & 0 \\ 0 & -P & 0 & 0 \\ 0 & 0 & -P & 0 \\ 0 & 0 & 0 & E \end{pmatrix} \quad (7)$$

is relevant, where  $P$  is the pressure and  $E$  is the energy density.

Four EFEs (2)–(5) contain four quantities,  $\lambda$ ,  $\nu$ ,  $P$ , and  $E$ , which are the functions of variable  $r$  in the considered static case. However, when the components of tensor (7) are supplied into EFEs (2)–(5), then EFE (3) is identical with EFE (4). It means that we have only three equations, in fact, but these still contain four unknown quantities. We need to supply one more equation to solve the system. Usually, this additional equation is an equation of state (EoS) relating  $P$  and  $E$ . In Sect. 4.6, we however mention other kind of equations which can be assumed and added to complete the system.

Oppenheimer & Volkoff (1939) replaced the auxiliary function  $\lambda$  by other metric function they denoted  $u$ . This function was defined by

$$u = \frac{1}{2}r \left( 1 + \frac{1}{g_{rr}} \right) = \frac{1}{2}r (1 - e^{-\lambda}). \quad (8)$$

In this context, we see that  $u$  is another parameter characterizing the space-time. With the help of all, Eq.(8), matrix (7), and after an algebraic handling, EFEs (2) and (5) can be re-written to the form

$$\nu' = \frac{2}{r^2 - 2ru} \left( \frac{1}{2}\kappa Pr^3 + u \right), \quad (9)$$

$$u' = \frac{1}{2}\kappa Er^2. \quad (10)$$

Using the last three equations and Eq.(3) or identical Eq.(4) after  $T_2^2 = T_3^3 = -P$  is supplied, we can also express the derivative of pressure in respect to  $r$ , specifically

$$P' = -\frac{E + P}{r^2 - 2ru} \left( \frac{1}{2}\kappa Pr^3 + u \right) \quad (11)$$

or, taking into account relation (9),

$$P' = -\frac{E + P}{2}\nu'. \quad (12)$$

## 2.2. Equation of state - examples

In view of our explanation, we consider an example in which the additional equation is the EoS of the cold, degenerated, Fermi-Dirac, neutron gas (Chandrasekhar, 1935), which was also used by Oppenheimer & Volkoff (1939) in their pioneering work. The EoS can be derived from the integrals known within the quantum statistics for the number density,  $n_n$ , pressure,  $P$ , and energy density,  $E$ . These integrals can be found in the textbooks (e.g. Hansen & Kawaler, 1994). In course to calculate them, the authors used an auxiliary quantity,  $\tau$ , which is the function of the Fermi impulse,  $p_f$ , and is defined as

$$\tau = 4 \ln \left[ \frac{p_f}{m_n c} + \sqrt{1 + \left( \frac{p_f}{m_n c} \right)^2} \right], \quad (13)$$

where  $m_n$  is the mass of a neutron. With the help of  $\tau$ , the pressure and energy density can be given as

$$P = \frac{m_n^4 c^5}{96\pi^2 \hbar^3} \left( \sinh \tau - 8 \sinh \frac{\tau}{2} + 3\tau \right), \quad (14)$$

$$E = \frac{m_n^4 c^5}{32\pi^2 \hbar^3} (\sinh \tau - \tau). \quad (15)$$

$\hbar$  is the Planck constant divided by  $2\pi$ . In the EFEs,  $P$  and  $E$  are, thus, replaced with the single quantity  $\tau$  and it is useful to replace Eq.(11), giving the derivative of pressure in respect to  $r$ , with the equation (Oppenheimer & Volkoff, 1939)

$$\tau' = -4 \frac{\sinh \tau - 2 \sinh \frac{\tau}{2}}{r^2 - 2ru} \cdot \frac{\frac{m_n^4 c G}{24\pi \hbar^3} r^3 \left( \sinh \tau - 8 \sinh \frac{\tau}{2} + 3\tau \right) + u}{\cosh \tau - 4 \cosh \frac{\tau}{2} + 3}, \quad (16)$$

which gives the derivative of  $\tau$  in respect to  $r$ . Eq.(16) was derived from Eq.(11) realizing that  $dP/dr = (dP/d\tau)(d\tau/dr)$  and  $dP/d\tau$  was calculated deriving (14) in respect to  $\tau$ .

If the derivatives in respect to  $r$  in Eq.(12) are replaced with the differentiation in respect to  $\tau$  and relations (14) and (15) are used, we obtain the equation

$$\begin{aligned} & \left( \cosh \tau - 4 \cosh \frac{\tau}{2} + 3 \right) d\tau = \\ & = -\frac{1}{2} \left( 4 \sinh \tau - 8 \sinh \frac{\tau}{2} \right) d\nu, \end{aligned} \quad (17)$$

which can be analytically integrated. The integration yields a useful relation between the  $g_{tt}$  component of metric tensor and  $\tau$ ,

$$e^\nu = \frac{C_\nu}{\cosh \frac{\tau}{2} + 1}, \quad (18)$$

where  $C_\nu$  is an integration constant.

Besides the EoS expressed with the help of relations (14) and (15), we also consider the EoS in the form of a polytrope, EoS of radiation, or a combination of both. The polytrope can be given with the help of relations (Tooper, 1965)

$$P = K_P \rho^{1+1/N}, \quad (19)$$

$$E = NP + c^2 \rho, \quad (20)$$

where  $K_P$  is a constant of proportionality,  $\rho$  is the material density, and  $N$  is the polytrope index. The EoS of radiation is

$$E = 3P \quad (21)$$

and the EoS, which is the combination of a polytrope and radiation can be given as

$$P = K_P \rho^{1+1/N} + \frac{1}{3} a T^4 \quad (22)$$

and with  $E$  given by relation (20), again (but this time,  $P$  is given by relation (22), not by (19)). In Eq.(22),  $a$  is the radiation constant and  $T$  is the temperature related to material density, in the given context, as

$$T = T_{max} \left( \frac{\rho}{\rho_{max}} \right)^{1/N}. \quad (23)$$

$T_{max}$  and  $\rho_{max}$  are the constants, which equal to the maximum temperature and maximum density, respectively.

### 3. Acceleration of a test particle in rest, in GR

#### 3.1. Acceleration in the field of a point-like massive particle

In course toward understanding of an RCO configuration in the form of a hollow sphere, we remind (Neslušan, 2019) and analyze the formula giving the gravitational acceleration of a test particle (TP) in the vicinity of a point-like material object. The TP is in rest in respect to the object. To calculate its acceleration within GR, the equation of geodesic,

$$\frac{d^2 x^\alpha}{ds^2} = -\Gamma_{\beta\gamma}^\alpha \frac{dx^\beta}{ds} \frac{dx^\gamma}{ds}, \quad (24)$$

should be used.  $x^\alpha$  ( $\alpha = 1, 2, 3, 4$ ) are the four-coordinates and  $\Gamma_{\beta\gamma}^\alpha$  are the Christoffel symbols. Using relation  $dx^\alpha/ds = (dx^\alpha/dt)(dt/ds)$  (see, e.g., Straumann, 2013, p. 59), equation (24) can be re-written as

$$\frac{d^2 x^\alpha}{dt^2} = \left( \Gamma_{\beta\gamma}^\alpha \frac{dx^\beta}{dt} \frac{dx^\gamma}{dt} - \Gamma_{\beta\gamma}^\alpha \right) \frac{dx^\beta}{dt} \frac{dx^\gamma}{dt}. \quad (25)$$

In the considered spherical coordinate frame centered on the material object, the TP accelerates in the negative sense of the radial axis. The radial component of the acceleration is

$$\begin{aligned}
 \frac{d^2 r}{dt^2} &= (-\Gamma_{11}^1 + \Gamma_{14}^4 + \Gamma_{41}^4) \left(\frac{dr}{dt}\right)^2 - \Gamma_{22}^1 \left(\frac{d\vartheta}{dt}\right)^2 - \\
 &\quad - \Gamma_{33}^1 \left(\frac{d\varphi}{dt}\right)^2 - c^2 \Gamma_{44}^1 = \\
 &= \left(-\frac{1}{2} \frac{d\lambda}{dr} + \frac{d\nu}{dr}\right) \left(\frac{dr}{dt}\right)^2 + r e^{-\lambda} \left(\frac{d\vartheta}{dt}\right)^2 + \\
 &\quad + r \sin^2 \vartheta e^{-\lambda} \left(\frac{d\varphi}{dt}\right)^2 - \frac{c^2}{2} e^{\nu-\lambda} \frac{d\nu}{dr}, \tag{26}
 \end{aligned}$$

For the TP being in rest, i.e. with  $dr/dt = d\vartheta/dt = d\varphi/dt = 0$ , the last formula reduces to

$$\frac{d^2 r}{dt^2} = -c^2 \Gamma_{44}^1 = -\frac{c^2}{2} e^{\nu-\lambda} \frac{d\nu}{dr}. \tag{27}$$

Assuming that the object and the TP are in vacuum, the metrics in the vicinity of the object must be, according to the Birkhoff theorem (Birkhoff & Langer, 1923), the outer Schwarzschild metrics (OSM) (Schwarzschild, 1916). We know that this metrics was found as the solution of the EFEs in the case of spherical symmetry. Hence, only the diagonal components of the metric tensor are non-zero. We remind that we denoted them (in Sect. 2.1) as  $g_{11} = g_{rr}$ ,  $g_{22} = g_{\vartheta\vartheta}$ ,  $g_{33} = g_{\varphi\varphi}$ , and  $g_{44} = g_{tt}$ . In the OSM, components  $g_{\vartheta\vartheta}$  and  $g_{\varphi\varphi}$  are the same as in the flat space-time; specifically,  $g_{\vartheta\vartheta} = -r^2$  and  $g_{\varphi\varphi} = -r^2 \sin^2 \vartheta$ . Components  $g_{rr}$  and  $g_{tt}$  equal

$$g_{tt} = -\frac{K_\nu}{g_{rr}} = e^\nu = -K_\nu e^{-\lambda} = K_\nu \left(1 - \frac{2u_c}{r}\right), \tag{28}$$

where  $K_\nu$  and  $u_c$  are the integration constants (Equation (3) is the differential equation of the second order, therefore its solution must contain two integration constants). In the application like in our case, there is a convention to choose  $K_\nu = 1$ . If  $e^\nu$  and  $e^{-\lambda}$ , expressed by Eq.(28), are supplied into Eq.(27), then the acceleration of the TP is

$$\ddot{r} = -\left(1 - \frac{2u_c}{r}\right) \frac{c^2 u_c}{r^2} = -\frac{c^2 u_c}{r^2} + \frac{2c^2 u_c^2}{r^3}, \tag{29}$$

whereby the minus (plus) sign at the right-hand side indicates its orientation in the direction toward (outward from) the origin of coordinate frame. The double dot above  $r$  denotes the second time derivative of the radial distance,  $r$ .

### 3.2. Calibration of constant $u_c$

In a weak gravitational field, the Newton physics well describes the reality and, thus, the relations derived within GR should converge, in the limit of weak field, to the corresponding relations in the Newtonian physics. In the weak field,  $2u_c/r \ll 1$  and can be neglected. Then, the acceleration (29) reduces to

$$\ddot{r} = -\frac{c^2 u_c}{r^2}, \quad (30)$$

which is identical to the acceleration calculated by using the Newton gravitational law,

$$\ddot{r} = -\frac{Gm}{r^2}, \quad (31)$$

when the constant  $u_c$  equals

$$u_c = \frac{Gm}{c^2}. \quad (32)$$

In the last relations,  $m$  is the mass of a massive object in the Newtonian physics. It is worth stressing that this physics and GR are two conceptually different theories. Hence, the concept of mass in the former is completely different than the mass in the latter. In the former, the mass is not related to energy. We discuss the meaning of quantity  $u$  more in Sect. 5.2.

We note that constant  $u_c$  is, in fact, function  $u$  (see Sect. 2.1 and relation (8)) in the vacuum. Namely, we have  $E = 0$  in the vacuum and, according to relation (10),  $u' = 0$ , then. After the integration of this differential equation, we obtain  $u = u_c$ .

We see that the relativistic acceleration given by relation (29) consists of two terms. The first term,  $-c^2 u_c/r^2$ , is identical, in fact, to the acceleration in the Newtonian physics and we will refer to it as to the ‘‘Newtonian term’’. The second term,  $+2c^2 u_c^2/r^3$ , occurs in the GR formula for the acceleration. It is the ‘‘relativistic term’’. Interestingly, the sign of the relativistic term is opposite to that of the Newtonian term. Hence, the relativistic term is a repulsive contribution to the Newtonian gravitational attraction. Since the inequality  $2u_c/r < 1$  is always valid above the event horizon, the total gravitational acceleration must be attractive.

However, when we calculate the acceleration according to (i) the Newtonian formula (31) and (ii) relativistic formula (29) for the same system of particles and in the same configuration, then the absolute value of the first acceleration is greater than that of the second. In other words, the Newtonian gravity is stronger than the relativistic gravity above the event horizon.

If the whole massive object were located below its event horizon and also the TP were below this horizon, then, interestingly, its acceleration would be oriented away from the object; by formula (29), the gravitational action is implied to be repulsive below the horizon. No part of the RCO presented in this work is, however, located there.



### 3.3. Acceleration inside the spherically symmetric shell

This paper introduces the models of RCO in the form of a hollow sphere, with the inner physical surface and vacuum void inside. The example of such a model is given in Sect. 4. It may seem to be a paradox that the gravity, with its attractive character, shapes a spherically symmetric object to such a form. In this sub-section, we clarify the mechanism leading to an occurrence of the outward oriented acceleration in the deep RCO interior due to the gravitational attraction.

Because of simplicity of our explanation, we consider a thin, spherically symmetric material shell. It is well-known that the acceleration due to the net gravity of the shell is zero in the classical, Newtonian physics (this fact is also shown below). In GR, it is postulated that the metrics in the shell's interior must be the Minkowski metrics, which also implies the zero acceleration. However, this postulate is in a disagreement with the relativistic formula for the acceleration derived on the basis of the equation of geodesic. Thus, it is also in a disagreement with the EFEs.

Since we want to discuss the relevance of the old and new concepts of the RCO, we ignore the postulating the Minkowski metrics and use the above-found formula for the acceleration to derive the net acceleration in a spherical shell, in this sub-section. If the equation of geodesic is taken into account, then one can notice an important consequence of the relativistic term in the formula giving the acceleration on a TP inside the shell.

So, let us consider a thin, spherically symmetric, material shell. The density of matter in the shell is constant and equal to  $\rho$ . Let the gravity due to the matter in the shell be weak, therefore we can proceed, in our derivation, as in within the Newtonian physics. To describe the acceleration of TP, we further consider the rectangular coordinate frame  $O(xyz)$  with the origin identical with the position of the TP (Fig. 2). The center of the shell is situated on the negative part of the coordinate  $z$ -axis and its distance from the TP is smaller than the radius of the shell.

As seen in Fig. 2, the coordinate  $x$ - $y$  plane intersects the shell dividing it to the upper and lower globular canopies (the cross-curve of this plane with the shell is shown with the ellipse in Fig. 2; the center of the ellipse is identical to the position of the particle). Firstly, we calculate the partial acceleration of the TP due to the gravity of the matter in an infinitesimally small volume of the shell,  $dV_1$ , in the upper canopy. The volume is seen from the position of the particle under space angle  $d\Omega = \sin\vartheta d\vartheta d\varphi$  and the mass inside this volume is  $\mu_1 = \rho r_1^2 d\Omega dr$ . Symbol  $r_1$  stands for the distance between the volume and the TP.

It is worth characterizing the position of the TP also in the rectangular frame  $O(\tilde{x}_1\tilde{y}_1\tilde{z}_1)$  with the origin identical with the position of volume  $dV_1$  and the axes  $\tilde{x}_1$ ,  $\tilde{y}_1$ , and  $\tilde{z}_1$  parallel with  $x$ ,  $y$ , and  $z$ , respectively (Fig. 2). In this frame, the

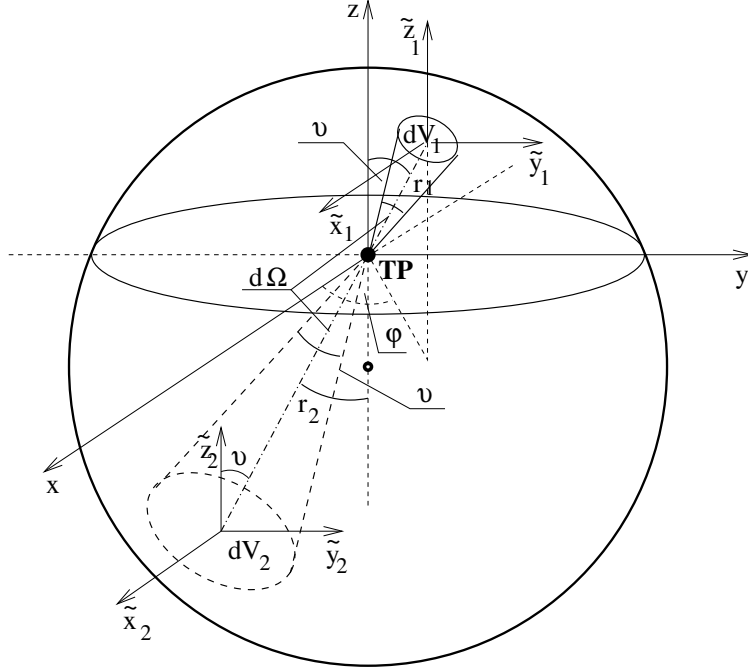


**Figure 2.** The scheme illustrating the position of a test particle (TP) inside a thin material shell (the large circle) and positions of two considered small partial volumes of the sphere,  $dV_1$  and  $dV_2$  (small ellipses). In Sect. 3.3, this scheme is used to explain the acceleration of the TP due to the matter of each of these volumes. In the explanation, three coordinate frames,  $O(xyz)$ ,  $O(\tilde{x}_1\tilde{y}_1\tilde{z}_1)$ , and  $O(\tilde{x}_2\tilde{y}_2\tilde{z}_2)$ , are considered. From the position of the particle, volume  $dV_1$  is seen under the same space angle,  $d\Omega$ , as volume  $dV_2$ . The particle is located in the origin of the frame  $O(xyz)$ . The origins of frames  $O(\tilde{x}_1\tilde{y}_1\tilde{z}_1)$  and  $O(\tilde{x}_2\tilde{y}_2\tilde{z}_2)$  are identical with the positions of volumes  $dV_1$  and  $dV_2$ , respectively, and their axes are parallel with the corresponding axes of  $O(xyz)$  frame. The whole shell is divided by the coordinate  $x$ - $y$  plane (the cross-curve of both the plane and the shell is the ellipse with the horizontal axis passing through the TP), into upper and lower globular canopies. Volume  $dV_1$  is situated in the upper and  $dV_2$  in the lower canopy.

position of the TP can be characterized with the radial distance  $\tilde{r}_1 = r_1$  and angles  $\tilde{\vartheta}_1 = \pi + \vartheta$ ,  $\tilde{\varphi}_1 = \varphi$ .

Let us ignore, for a while, the remaining part of the shell and consider only the TP and the matter in the volume. The infinitesimally small volume can be regarded as a point and the metrics in its vicinity is the OSM. It means that the parameter  $u_c$  can be given with the help of mass  $\mu_1$  as  $u_1 = G\mu_1/c^2$ . We describe the OSM metrics and corresponding acceleration of the TP in the

rectangular coordinate frame  $O(\tilde{x}_1\tilde{y}_1\tilde{z}_1)$ . The  $\tilde{z}_1$ -component of the acceleration of the TP due to the matter in the volume is given by

$$\ddot{\tilde{z}}_1 = - \left( 1 - \frac{2G\mu_1}{r_1} \right) \frac{G\mu_1}{\tilde{r}_1^2} \frac{\tilde{z}_1}{\tilde{r}_1} \quad (33)$$

(see, e.g., our earlier paper (Neslušan, 2023), where we derived the  $x$ -component of the acceleration; the formulas for the other components are analogous; these can be obtained by the cyclic interchange of spatial variables,  $x \rightarrow y \rightarrow z \rightarrow x$ ).

Obviously,  $\tilde{z}_1/\tilde{r}_1 = \cos \vartheta_1$  and since  $\vartheta_1 = \pi - \vartheta$ , we can write  $\tilde{z}_1/\tilde{r}_1 = \tilde{z}_1/r_1 = -\cos \vartheta$  (Fig. 2). Because the  $z$ -coordinate is related to  $\tilde{z}_1$  as  $z = \tilde{z}_1 + r_1 \cos \vartheta$ , then  $z$ -components of corresponding accelerations are related as  $\ddot{z} = \ddot{\tilde{z}}_1$  (the position of volume  $dV_1$  does not change in time, therefore  $r_1$  and  $\vartheta$  are not functions of time). Using these relations and  $\mu_1 = \rho r_1^2 \sin \vartheta d\vartheta d\varphi dr$ , relation (33) can be re-written as

$$\begin{aligned} \ddot{\tilde{z}}_1 = & G\rho \cos \vartheta \sin \vartheta d\vartheta d\varphi dr - \\ & - \frac{2G^2\rho^2}{c^2} r_1 \cos \vartheta (\sin \vartheta d\vartheta d\varphi dr)^2, \end{aligned} \quad (34)$$

where  $\ddot{\tilde{z}}_1$  is the acceleration of the TP due to volume  $dV_1$  referred in the  $O(xyz)$  frame.

Secondly, let us consider the matter in the infinitesimal volume of the shell,  $dV_2$ , in the exactly opposite direction than the first volume (Fig. 2). Also the second volume is seen from the position of the TP under space angle  $d\Omega$ . When we calculate the acceleration of the TP, the volume can be regarded as a point-like massive particle with the neighboring metrics being the OSM. Now, we describe the metrics and corresponding acceleration in the third rectangular coordinate frame  $O(\tilde{x}_2\tilde{y}_2\tilde{z}_2)$  with the origin identical with the position of  $dV_2$  and axes parallel with the axes of the  $O(xyz)$  frame. In  $O(\tilde{x}_2\tilde{y}_2\tilde{z}_2)$ , the position of the TP is characterized by radial distance  $\tilde{r}_2 = r_2$  and with angles  $\vartheta_2 = \vartheta$  and  $\varphi_2 = \pi + \varphi$ .

The  $\tilde{z}_2$ -component of the acceleration of the TP due to the gravity of matter in  $dV_2$  can again be calculated by using relation (33) with the interchanges  $\tilde{z}_1 \rightarrow \tilde{z}_2$ ,  $\tilde{r}_1 \rightarrow \tilde{r}_2$ , and  $\mu_1 \rightarrow \mu_2$ . Therefore, the mass of  $dV_2$  equals  $\mu_2 = r_2^2 d\Omega dr$  and  $u_c$  in the OSM can be expressed as  $u_2 = G\mu_2/c^2$ . Now  $\tilde{z}_2/\tilde{r}_2 = \tilde{z}_2/r_2 = \cos \vartheta$  and the relation for the acceleration in the case of  $dV_2$  can be given as

$$\begin{aligned} \ddot{\tilde{z}}_2 = & -G\rho \cos \vartheta \sin \vartheta d\vartheta d\varphi dr + \\ & + \frac{2G^2\rho^2}{c^2} r_2 \cos \vartheta (\sin \vartheta d\vartheta d\varphi dr)^2 \end{aligned} \quad (35)$$

in the  $O(xyz)$  frame (it is valid  $z = \tilde{z}_2 - r_2 \cos \vartheta$  and, hence,  $\ddot{z} = \ddot{\tilde{z}}_2$ ).

The first, Newtonian, term in (35) has the same size, but opposite sign than this term in (34), therefore the sum of the Newtonian terms in both components

of the acceleration,  $\ddot{z}_1$  and  $\ddot{z}_2$ , is zero. This is valid not only for the two considered infinitesimal volumes, but for every pair of volumes of which the first is located in the upper and the second one in the opposite direction in the lower globular canopy. The partial Newtonian gravity of the first volume is always eliminated by the partial Newtonian gravity of the second volume, which is seen under the same space angle. As we already mentioned, the resulting net gravity in the shell is zero in the Newtonian physics.

However, the sum of the relativistic terms is not zero. We have

$$\ddot{z}_1 + \ddot{z}_2 = \frac{2G^2\rho^2}{c^2}(r_2 - r_1) \cos\vartheta(\sin\vartheta d\vartheta d\varphi dr)^2. \quad (36)$$

Angle  $\vartheta$  characterizes the position of volume  $dV_2$  in the lower globular canopy, therefore it ranges from zero to  $\pi/2$  and  $\cos\vartheta > 0$ . It is also valid that  $r_1 < r_2$  (see Fig. 2), i.e.  $r_2 - r_1 > 0$ , therefore the total acceleration, due to the combined action of both volumes, is  $\ddot{z}_1 + \ddot{z}_2 > 0$ .

The positive value of the acceleration means that its  $z$ -component, in the  $O(xyz)$  coordinate frame, is oriented in the positive direction of the coordinate  $z$ -axis. This is, again, valid for each pair of volumes, the first in the upper and the second in the lower globular canopy, which are seen from the position of the TP under the same space angle. Taking into account all possible pairs of volumes, summarily, we deduce that the net acceleration due to the gravity of matter in the upper canopy is larger than the net acceleration due to the gravity of matter in the lower canopy (Neslušan, 2019, see especially Fig. 7b). It means that the TP is accelerated away from the center of the shell. However, we would like to stress, again, that the TP is not *repelled* from the shell's center; it is attracted by the matter of the upper globular canopy with a stronger gravity, which dominates over a weaker gravity of the lower globular canopy.

It is well known that GR is not a linear theory, therefore our explanation described above is valid only for a weak field. In a strong field, the first result of our deduction, i.e. the acceleration for the system "matter in the 1-st volume"- "test particle", is no longer valid after the "matter in the 2-nd volume" is added to this system. In GR, the partial accelerations cannot be given as a simple vectorial sum as in the Newtonian physics. We presented the explanation valid, approximately, for a weak field in the sake of its transparency of the operating mechanism.

The generally correct way to calculate the acceleration in the shell is solving the EFEs as it was made in the construction of an example of a neutron star, which is presented later, in Sect. 4.1. However, the effect of the outward oriented gravitational action is not, then, very transparent. The resulting solution of the numerical integration of the EFEs is discussed more in the following section. Anyway, the explanation given in the text above indicates that the gravitational acceleration of a TP in the interior of a spherical layer of RCO matter is non-zero and oriented outward in GR.

## 4. Example of RCO

### 4.1. Modeling of RCO

A simple model of a neutron star can be created solving field equations (9), (10), and (16), in which  $P$  and  $E$  are expressed with the help of (14) and (15). Equations (9), (10), and (16) contain three quantities,  $\nu$ ,  $u$ , and  $\tau$ , which are functions of a single variable  $r$ ; the system can be solved.

An analytical solution of these equations is unknown, therefore one can solve them via a numerical integration. The integration cannot start in the object's center, in  $r = 0$ , since the denominator  $r^2 - 2ru \rightarrow 0$  for  $r \rightarrow 0$  in the fractions in Eqs.(9) and (16). The integration must start in a finite star-centric distance.

Researchers who modeled neutron stars usually started the integration at a small star-centric distance  $\Delta r$ . The integration was processed outward and terminated at the outer physical surface of the star where the pressure and energy density vanished. They assumed that all quantities acquired essentially the same value in the true center of the star (at  $r = 0$ ) as in the small starting distance  $\Delta r$ , since  $\Delta r$  could be, e.g., 1 cm. Hence, the assumption seems to be, intuitively, reasonable in the case of an object with  $\sim 10$  to  $\sim 15$  km radius.

It however appears that the human intuition fails in this case. If one starts the integration in a finite star-centric distance and performs it in two stages: stepping outward and inward, then the pressure and energy density vanish not only at the outer physical surface, but they, earlier or later, decrease and vanish in a non-zero star-centric distance in the inward processed integration as well. This fact implies the existence of an inner physical surface and vacuum void inside. In Sect. 4.2, we explain why the inner surface occurs in a gaseous object. In Sect. 4.6, we discuss some known solutions leading to a fulfilled-sphere RCO and explain why these solutions are irrelevant to the real gaseous RCOs.

In Fig. 3, there is the behavior of pressure in a model of a neutron star constructed by integrating Eqs.(9), (10), and (16) for the EoS given by relations (14) and (15). It is reasonable to start the integration in the distance,  $r_o$ , where the net gravity is zero (where  $\nu' = 0$ ) and also the pressure and energy density reach their maximum (where the function representing the pressure reaches a local extreme, i.e.  $P' = 0$ ). Seeing relations (9) and (11),  $\nu' = 0$  and  $P' = 0$  if  $(1/2)\kappa P_{max}r_o^3 + u_o = 0$ . From the latter

$$u_o = -\frac{1}{2}\kappa P_{max}r_o^3 \quad (37)$$

in the zero-gravity distance (Neslušan, 2017b). From this point, the integration should be done in two stages, stepping inward and outward. The maximum pressure,  $P_{max}$ , and the zero-gravity distance,  $r_o$ , are arbitrary input parameters. One can vary their values to obtain the model of an object with the required mass and the outer (or inner) radius.

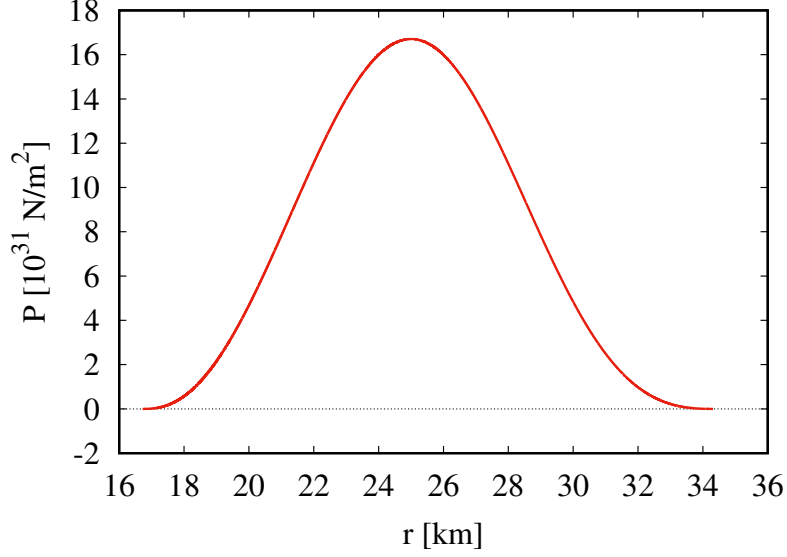


**Figure 3.** The dependence of the pressure,  $P$ , on the radial distance,  $r$ , from the center of the star in the example of a neutron star presented in Sect. 4. The zero-gravity distance in this object is  $r_o = 25$  km. Its inner and outer radii equal 16.7 and 34.4 km, respectively.

#### 4.2. Distribution of state quantities

When we proceed as described in the previous sub-section, we can construct a model of RCO - a neutron star. In the example with the result shown in Fig. 3, the distance of zero net gravity was chosen to be  $r_o = 25$  km and the rest energy in terms of the rest mass,  $M_o$ , was achieved, doing an iteration, to be  $M_o = 5 M_\odot$  (it corresponded to the Fermi impulse in  $r_o$  equal to  $0.27464 m_n c$ ). We remind that the rest mass is given by the formula (e.g. Straumann, 2013; Misner et al., 2017, but with  $R_{in} \equiv 0$ , there)

$$M_o = 4\pi m_n \int_{R_{in}}^{R_{out}} n_n r^2 \sqrt{-g_{rr}} dr, \quad (38)$$

where  $n_n$  is the number density of neutrons. It can be calculated as (Oppenheimer & Volkoff, 1939)

$$n_n = \frac{1}{3\pi^2} \left( \frac{m_n c}{\hbar} \right)^3 \sinh^3 \frac{\tau}{2}. \quad (39)$$

As seen in Fig. 3, the pressure decreases outward as well as inward from  $r_o$ . The stability of the object is kept by a balance between the gravity and the

gradient of pressure. Let us analyze the net gravitational acceleration in more detail. When one divides the RCO into a large number of thin concentric layers and considers a radius  $r$ , there is a certain number,  $N_l$ , of spherical layers with radii smaller than  $r$  (“lower” layers) and a certain number,  $N_u$ , of spherical layers with radii larger than  $r$  (“upper” layers). Obviously, all the lower layers attract a TP in distance  $r$  downward, toward the RCO center, and the upper layers attract it outward as indicated in Sect. 3.3.

Let the TP be initially located at such a distance  $r$  that the net acceleration due to the lower layers is larger than that due to the upper layers, therefore the particle is accelerated inward. If we consider the particle at a smaller  $r$  than initially, the number of lower layers is smaller and the number of upper layers larger. Correspondingly, the net gravity of lower layers is reduced and that of upper layers magnified. If we further reduce  $r$ , then there must occur a critical distance,  $r_o$ , in which the absolute value of the net acceleration of lower layers just equals the absolute value of the net acceleration of upper layers. The total net gravity is, thus, zero in this distance. In distances  $r < r_o$ , the outward oriented net acceleration due to the upper layers must prevail; the particle accelerates outward in this region.

It seems that the region of the outward oriented gravity must exist in every gaseous RCO. Let us perform the following deduction. Imagine an RCO with both the inner radius and the zero-gravity distance approaching zero. In such an RCO, the mass within the sphere of radius  $r_o$  approaches zero when  $r_o \rightarrow 0$  and, thus, the net gravity of the lower layers must also approach zero. This very low net gravity must be overcome by the net gravity of the upper layers before  $r_o$  reaches the exact zero value, because the acceleration due to this gravity approaches a finite (i.e. greater than zero) constant when  $r_o \rightarrow 0$ . This deduction would surely be correct in the flat space-time of Newtonian physics. However, the geometry of curved space-time is more difficult and we cannot exclude that the net gravity of the upper layers does not dominate even in the exact center of RCO.

The problem of existence or non-existence of the solution implying a realistic fulfilled-sphere RCO model could be solved with the help of an analytical solution of the EFEs for a realistic EoS. In physics, such a solution is often searched for in the form of Taylor series. Actually, we can find the coefficients of the series for  $P$ ,  $E$ , and  $u$  in the vicinity of the center. However, the individual terms are so complicated that it is practically impossible to prove a convergence of the series.

In a stable RCO, the gravity is balanced by the gradient of pressure. In region  $r > r_o$ , the gravity acting on each concentric layer is oriented inward and the gradient of pressure, being the same size as the gravity, pushes the layer outward (notice the decrease of the pressure with the increasing radial distance in this region in Fig. 3). In region  $r < r_o$ , the orientation of the forces is opposite: the gravity acts outward and gradient of pressure inward (the pressure increases with the increasing radial distance, here).

### 4.3. Behavior of metrics

The behavior of the quantities  $g_{rr}$ ,  $g_{tt}$ , and  $u$  characterizing the metrics in our example of RCO is shown in Fig. 4. In a realistic model of a neutron star or any realistic RCO, the metrics of the RCO body must be smoothly tailored to the external, vacuum metrics. (We use the term ‘‘RCO body’’ to refer to the volume inside the RCO, between the RCO-centric spheres with radii  $R_{in}$  and  $R_{out}$ .) According to the Birkhoff theorem (Birkhoff & Langer, 1923), the vacuum metrics in the vicinity of a spherically symmetric distribution of matter must be the OSM. Actually, as demonstrated in Fig. 4, only this metrics can be smoothly tailored to the metrics of the object’s body. The behavior of the RCO-body metrics is shown with the thick blue curve in each panel of the figure. The OSM in both outer (green curves) and inner (purple curves) physical surfaces actually touches the RCO-body metrics at the end points of the blue curve and the corresponding OSM curve smoothly continues behind the corresponding end point; there is no break in the merged curve. It means that the corresponding derivatives in respect to  $r$  equal each other; this was verified making a numerical calculation of the derivatives.

In Fig. 4c, notice that function  $u < 0$  below the distance  $r_z$ , whereby  $R_{in} < r_z < R_{out}$ . The negative  $u$  occurs in the central region of the RCO body as well as in the internal vacuum void of any numerically created model of the RCO consisting of a comprehensible perfect fluid.

In the OSM, the function  $u$  is a constant. In the region  $r < R_{in}$ , we denote this function by  $u_{in}$  (the purple straight line in Fig. 4c) and in  $r > R_{out}$  by  $u_{out}$  (the green straight line). The OSM  $g_{rr}$  component of metric tensor can be tailored to the  $g_{rr}$  of the RCO body at distances  $r = R_{in}$  and  $r = R_{out}$ . The OSM  $g_{rr}$  equals  $g_{rr} = -1/(1 - 2u_{in}/r)$  in the region  $r \leq R_{in}$  (the purple curve in Fig. 4a) and  $g_{rr} = -1/(1 - 2u_{out}/r)$  in the region  $r \geq R_{out}$  (the green curve in Fig. 4a). Similarly, the  $g_{tt}$  component of the OSM can be tailored to  $g_{tt}$  of the RCO body at distances  $R_{in}$  and  $R_{out}$  and can be calculated as  $g_{tt} = K_{\nu,i}(1 - 2u_{in}/r)$  in the region  $r \leq R_{in}$  (the purple curve in Fig. 4b) and  $g_{tt} = K_{\nu,o}(1 - 2u_{out}/r)$  in  $r \geq R_{out}$  (the green curve).

There is a convention to put  $K_{\nu,o} = 1$ . Since the whole behavior of  $g_{tt}$ , from  $r = 0$  to  $r = \infty$ , is fixed by this calibration, the constant  $K_{\nu,i}$  cannot be chosen arbitrarily. It can be calculated on the basis of relation (18). At the inner and outer RCO surfaces, the pressure and energy density vanish, therefore the corresponding Fermi impulse equals zero in  $R_{in}$  and  $R_{out}$ . Then, according to (13), also  $\tau = 0$  at these two distances. For  $\tau = 0$ ,  $g_{tt}(R_{in}) = C_\nu/2$  as well as  $g_{tt}(R_{out}) = C_\nu/2$ , therefore  $g_{tt}(R_{in}) = g_{tt}(R_{out})$ , according to (18). Notice that the component  $g_{tt}$  inside the RCO-body (the blue curve in Fig. 4b) begins and ends at the same value. It means that  $K_{\nu,i}(1 - 2u_{in}/R_{in}) = K_{\nu,o}(1 - 2u_{out}/R_{out})$  or (Neslušan, 2015)

$$K_{\nu,i} = \frac{1 - \frac{2u_{out}}{R_{out}}}{1 - \frac{2u_{in}}{R_{in}}}, \quad (40)$$



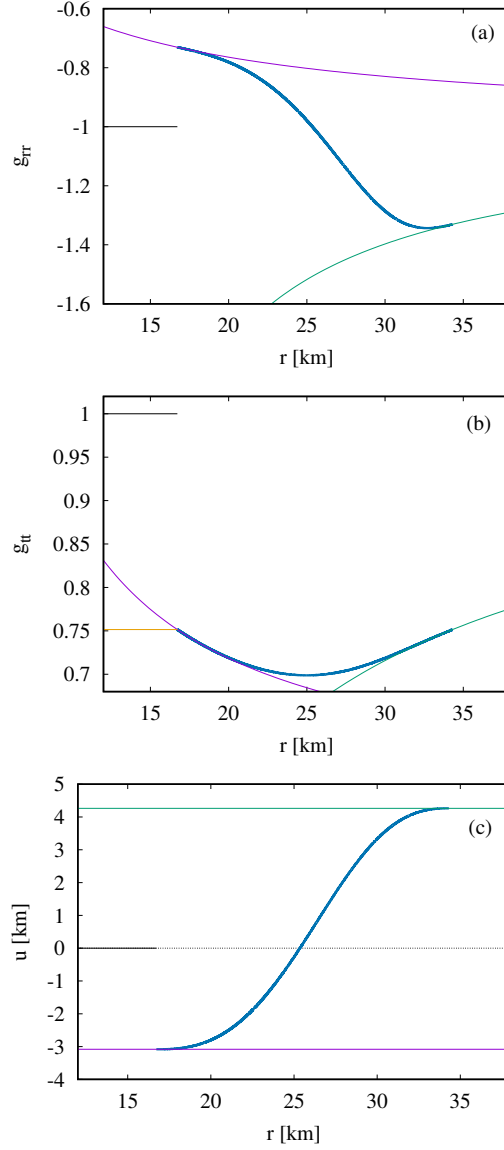


**Figure 4.** The dependence of  $g_{rr}$  (panel a) and  $g_{tt}$  (b) components of the metric tensor, as well as the auxiliary function  $u$  (c) on the radial distance,  $r$ , in the example of the neutron star presented in Sect. 4. The metrics in the star’s body is shown with the thick blue curve. The OSM, which can tailored to the RCO-body metrics at the outer (inner) physical surface in the right-hand end (left-hand end) of the thick blue curve, is shown with the thin green (thin purple) curve in each plot. The corresponding Minkowski metrics is shown with the black or orange straight line (see Sect. 4.4).

if we take into account the convention  $K_{\nu,o} = 1$ . In the example of a neutron star presented above,  $K_{\nu,i} = 0.549047$ .

An analogous equation to Eq.(18) can also be found for other EoSs than (14) and (15); probably for every reasonable EoS. For the polytrope (see relations (19) and (20)), in which  $E$  and  $P$  are functions of the material density,  $\rho$ , one can find

$$e^\nu = \frac{A_1}{(1 + A_2\rho^{1/3})^2}, \quad (41)$$

where  $A_1$  is an integration constant and  $A_2$  is a constant related to the maximum pressure and maximum material density of RCO. deLyra & Carneiro (2023) found the equation relating  $g_{tt}$  component and the energy density for other kind of a polytrope. Again,  $\rho = 0$  or  $E = 0$  in both  $R_{in}$  and  $R_{out}$ , therefore  $g_{tt}(R_{in}) = g_{tt}(R_{out})$  also in these cases. Likely, this equality is universal.

In the vacuum far from the star, i.e. at a distance  $r \gg R_{out}$ , the gravitational acceleration of a TP due to the star's gravity can be well approximated with the Newtonian formula

$$\ddot{r} = -\frac{GM_{out}}{r^2}, \quad (42)$$

in which the parameter  $u_{out}$  is again calibrated with the parameter  $M_{out}$ , which can be identified with the Newtonian mass of the object, whereby  $M_{out} = c^2 u_{out}/G$ . We established this new notation because we use  $M_{out}$  as the parameter within GR. As seen, it corresponds to  $u_{out}$ , which characterizes the vacuum metrics in the region of  $r \geq R_{out}$ . (Later, we use also notation  $M_{in} = c^2 u_{in}/G$  for the parameter corresponding with  $u_{in}$ , which characterizes the vacuum metrics in the region of  $r \leq R_{in}$ .)

Since the neutron star is the RCO with the GR gravity different from its Newtonian counterpart, acceleration (42) is not proportional to the mass  $M$  which is the equivalent of the total energy (see Sect. 5), but it is determined by the value  $M_{out}$  characterizing the metrics above the outer RCO surface. While the total mass, calculated within GR, is  $M = 4.97457 M_\odot$ , the Newtonian mass  $M_{out} = 2.88708 M_\odot$  in our example. When the experts spoke about the measured ‘‘mass’’ of a neutron star, they spoke about the quantity  $M_{out}$ , in fact. In the case of the given example, they would say that the *mass* is  $2.88708 M_\odot$  (not  $4.97457 M_\odot$ ). Unfortunately, the Newtonian and GR concepts of mass are often used in a confusing way in this context.

The actual energy content of all known neutron stars is still unknown. We can only guess that the true  $M$  is significantly larger than the measured  $M_{out}$ .<sup>1</sup> In our example, we can clearly see the essential difference between GR and Newtonian physics in the case of RCOs.

---

<sup>1</sup>Some models of the super-massive RCOs constructed with the EoS in the combined form of a polytrope and radiation imply that the total RCO mass as the equivalent of energy can exceed its Newtonian mass  $M_{out}$  by several orders of magnitude, so far. (Neslušan, 2022)

#### 4.4. A note on the Minkowski metrics inside a spherical shell

In the literature, we can find a claim that the space-time inside the spherical shell is described by the Minkowski metrics, which implies zero gravitational acceleration of a TP. Our deduction made in Sects. 3.3 and 4.2 however implies that this claim has the character of a postulate. In addition, the claim is in a disagreement with the Birkhoff theorem (Birkhoff & Langer, 1923) saying that the vacuum metrics in the vicinity of any spherically symmetric distribution of matter must be the OSM (with  $u_c \neq 0$ ; the Minkowski metrics can also be regarded as the special case of the OSM, with  $u_c = 0$ ).

To postulate the Minkowski, flat, metrics, in the RCO vacuum void, one must neglect the second term in relation (29). It means that the acceleration implied by the equation of geodesic is replaced with the acceleration by the Newton gravitational law, in fact. In other words, the equation of geodesics is ignored, therefore GR itself is ignored. The Minkowski metrics was postulated to achieve the regularity of metrics in the RCO's center (see Sect. 7.1). But it is not a very logical way, when one, in course to achieve the regularity within GR, must ignore this theory.

In addition, the Minkowski metrics  $(-1, -1, -1, 1)$  cannot be smoothly tailored with the metrics in the shell's body (Neslušan, 2017b) as is demonstrated in Fig. 4 (the black straight line in each panel). If the  $g_{tt}$  component of the Minkowski metrics equaled other constant than unity, the net gravity in the shell would also be zero. But even if we chose such a constant, which would lead to the linking of the Minkowski  $g_{tt}$  with the shell-body  $g_{tt}$  in  $R_{in}$  (this alternative Minkowski  $g_{tt}$  is drawn with orange color in Fig. 4b), the derivatives of both the orange straight line and the blue curve in  $R_{in}$  would not be equal. There would still be a discontinuity of the metrics. In conclusion, the postulate of the Minkowski metrics inside the spherical shell is physically unacceptable.

It is also unacceptable when we consider an infinitesimally thin shell. Then, the OSM relevant to the vacuum above the shell must be smoothly tailored with the Minkowski metrics in the shell's internal void. This is, however, impossible, since the derivatives  $dg_{rr}/dr$  and  $dg_{tt}/dr$  of the OSM are never zero at the shell's radius and, thus, they cannot match their Minkowski-metrics counterparts. The metrics that can be smoothly tailored to the RCO-body metrics at the inner surface of RCO is the OSM with a constant  $u_c < 0$  as we demonstrated in Sect. 4.3 (see especially Fig. 4).

#### 4.5. On the central singularity

As already mentioned, the metrics in the vacuum void below the RCO's inner surface is the OSM, but with  $u_c \equiv u_{in} < 0$  (Fig. 4c). The OSM has a singular point at  $r = 0$ , since  $g_{tt} \rightarrow \infty$  (not  $-\infty$  because  $u_{in} < 0$ ).

The inequality  $u_{in} < 0$  means that a TP in the void is accelerated outward from the RCO's center as it was indicated in Sect. 3.3 and modeled in Sect. 4.3.

This acceleration increases above all limits when  $r \rightarrow 0$ , but, because it is oriented outward, the singularity is the Big-Bang type singularity (Neslušan, 2019). Thus, it is not in a conflict with the cosmic censorship (Penrose, 1969).

The “repulsive” character of the singularity was also stated by deLyra et al. (2023) in the conclusions of their paper. We should however be careful when we use the adjective “repulsive”. It can be used for the sake of simplicity of language to express the “repulsive” (from the RCO’s center) orientation of the force field. When we however analyze the physical nature of the force action, we must realize that the point in the exact RCO’s center is a vacuum point having no influence on a TP in its vicinity. The active agent acting on the particle is the circumambient matter of the RCO, which *attracts* it away from the center. This attraction increases above all limits when  $r \rightarrow 0$  because of the geometry of space-time in the RCO’s internal vacuum void.

In reality, the mass of RCO-constituting matter is finite and a finite mass can be a source of only a finite action. Then, the singularity due to a finite action cannot be a true singularity. This claim can be supported by the following thought experiment (Neslušan, 2019). We shoot a particle situated in the internal RCO cavity toward the RCO center (singularity). If the kinetic energy of the particle is so small that its influence on the metrics in the cavity is negligible in comparison to that of the matter constituting the RCO, then the particle is decelerated, approaches the center up to a certain finite distance, where it is stopped, and then accelerated back by the gravity of the RCO matter.

On the contrary, if the energy of the particle is so high that the influence of this energy dominates over that of the RCO matter, then the metrics inside the vacuum void is re-configured. The presence of this high energy must have an impact on the neighboring space-time. After the re-configuration, the central singularity simply disappears. In such a case, the particle can pass through the point at  $r = 0$ , but this point is no longer a singular point. The experiment implies that the central singularity is only an abstract singularity, which figures in our mathematical description of the void metrics, but the singular point (until it remains singular) can never be visited by any material object and, hence, detected by any observer.

#### 4.6. Remarks on the fulfilled-sphere solutions

In the context of the hollow-sphere concept of RCO, it is necessary to mention some known solutions of the EFEs, which resulted in the objects without the inner radius (e.g. Tolman, 1939; Buchdahl, 1967; Whittaker, 1968).

In Sect. 2, we showed that EFEs (3) and (4) are identical and this circumstance reduces the number of equations in the system to three, but we have four unknown quantities. One equation must be supplied from outside of GR. Since there is no mathematical restriction, any equation, representing any definition, can be chosen. For example, Tolman (1939) assumed an ad hoc behavior of the auxiliary metric functions  $\lambda = \lambda(r)$  and  $\nu = \nu(r)$ , specifically  $e^{\nu}\nu'/(2r) = \text{const.}$

(Solution IV),  $e^\nu = \text{const.}$  (Solution V), or  $e^{-\lambda} = \text{const.}$  (Solution VI). Although such the additional assumption is only an author's fantasy, one can still obtain a toy model resulting from the mathematical solution of the EFEs.

Such a model is not, however, related to reality. It can answer the question of what would the internal structure of RCO look like if we assumed, e.g.,  $e^\nu \nu' / (2r)$  is equal to a constant. It is, however, questionable if the RCO model with such a structure could be applied to a real object. The fact that such the model is irrelevant to reality can be also seen from the discrepancy that a specific real RCO can be described by only one, unique, solution, but Tolman published seven various solutions and many other solutions were published by other authors. The behavior of no quantity in the RCO body can be guessed, when we deal with a model of a real object. From the point of view of physics, a correct way to solve the EFEs, in course to obtain a realistic model of RCO, is consideration of a realistic EoS, which is the input (the fourth equation) into the system of the EFEs. Then, solving the EFEs, one obtains a regular, realistic model of RCO.

As we argued in Sect. 4.1, the numerical modeling of RCO always implies an object in the form of a hollow sphere. An exception is an RCO consisting of the incomprehensible perfect fluid. The incomprehensibility implies a resistance of fluid against a deformation. Such the fluid would have a constant density,  $\rho$ , throughout the RCO's body. Several solutions of the EFEs applicable to the RCOs of this kind were found, e.g., the solution published by Schwarzschild (1916) or Solutions I–III by Tolman (1939). Nevertheless, the gravity is oriented outward in the innermost region also in the objects constructed on the basis of these solutions. The distribution of matter down to the center is caused by the incomprehensibility.

The objects described by the models with an artificially defined behavior of a quantity in their bodies, like that in the papers by, e.g., Tolman (1939); Buchdahl (1967), or Whittaker (1968), could, perhaps, be artificially constructed. However, they would have been constituted of a solid material, with a significant tensile strength. The strength, resisting a deformation of material, should be then taken into account and other stress-energy tensor than that for a perfect fluid, defined by relation (7), should have to be used. The stress-energy tensor (7) and corresponding EFEs (9)–(11) are not relevant to a solid matter. Hence, the solutions implying the fulfilled-sphere RCOs, published by the above-mentioned authors, are ruled out as contra-examples of the necessity of hollow-sphere configuration of gaseous RCOs.

Taking into account this circumstance, we are forced to state that no model of RCO, which would have been completely described (from RCO-centric distance  $r = 0$  to  $r = \infty$ ), has ever been constructed and published. This is in a contrast with the hollow-sphere models, one of which is just published in this paper and other models were published in our past papers as well as in the paper by other authors (the references to these papers are given in Sect. 1).

## 5. Energy of RCO

### 5.1. General formulas. Mass

In GR, the energy,  $W$ , of a static, spherically symmetric RCO can be calculated as the integral of energy density,  $E$ , through the RCO's volume, i.e. from its inner surface with radius  $R_{in}$  to its outer surface having radius  $R_{out}$ . Specifically (e.g. [Straumann, 2013](#); [Misner et al., 2017](#), but with  $R_{in} \equiv 0$ , there),

$$W = 4\pi \int_{R_{in}}^{R_{out}} r^2 E dr. \quad (43)$$

If we take into account EFE (10), the integrand  $r^2 E$  equals

$$r^2 E = \frac{2}{\kappa} \frac{du}{dr} = \frac{c^4}{4\pi G} \frac{du}{dr} \quad (44)$$

and relation (43) can be re-written as

$$W = \frac{c^4}{G} \int_{R_{in}}^{R_{out}} \frac{du}{dr} dr = \frac{c^4 u_{out}}{G} - \frac{c^4 u_{in}}{G} \quad (45)$$

where we denoted  $u(R_{in}) = u_{in}$  and  $u(R_{out}) = u_{out}$ . It appears that the inequalities  $u_{in} < 0$  and  $u_{out} > 0$  are always valid. Hence, the energy  $W = |c^4 u_{out}/G| + |c^4 u_{in}/G| > 0$ , i.e. the energy is positive.

### 5.2. A remark on quantity $u$ in the context of mass

As we stated in Sect. 3.2, the parameter  $u_c$  can be calibrated, after it is multiplied by the constant  $c^2/G$ , with the help of Newtonian mass. However, is the quantity  $u_c c^2/G$  really a mass? We know that each quantity in the unit of length multiplied by  $c^2/G$  becomes the quantity of the unit of mass. For example, a vector  $\mathbf{r} = (x, y, z)$  multiplied by  $c^2/G$  changes to  $\mathbf{m}_r = (m_x, m_y, m_z)$ , i.e. its components are quantities in the unit of mass. An object may be located at a position, where one or more of its components  $x$ ,  $y$ , or  $z$ , and, hence,  $m_x$ ,  $m_y$ , or  $m_z$  are negative. Can we say that the object cannot be in any such a position because a ‘‘mass’’ must not be negative? Of course, this would not be a reasonable demand. At the same time, we cannot demand that the negative values of the quantity  $uc^2/G$  must be forbidden.

In GR, the quantity  $uc^2/G$  cannot be regarded as a mass despite its unit, which is a unit of mass. Its different character can be demonstrated in the following deduction. Let us consider a small volume inside a neutron star body. (Here, it is not important whether we describe this star by the old, fulfilled-sphere RCO concept or by new, hollow-sphere concept.) Its energy,  $W$ , is the integral of energy density through this volume. Since  $E > 0$ , here,  $W > 0$  and also mass  $M = W/c^2 > 0$ . However, if we consider such a volume in the vacuum

above the outer surface,  $E = 0$  and, consequently its integral through the volume is zero, therefore  $M = W/c^2 = 0$ . But the space-time in the vacuum above the outer surface is curved; it is described by the OSM with the metric parameter  $u_c > 0$  and, hence,  $uc^2/G > 0$  in the place of the considered small volume. We see that  $uc^2/G$  cannot be mass. A quantity cannot be zero and non-zero at the same time.

In each realistic model of RCO that we or other authors created, the energy density was considered to be positive in any part of the RCO body. Therefore, its integral, corresponding energy as well as the corresponding mass were only positive (or zero in the vacuum below the inner and above the outer RCO surfaces). A negative value of  $uc^2/G$  in the region  $r < r_z$  of RCO is acceptable, since it is not a mass.

The metric quantity  $u$  is an alternative form of the  $g_{rr}$  component of the metric tensor (see relation (8)). If  $u \geq 0$ , then  $g_{rr}$  ranges from  $-\infty$  to  $-1$ . However, one can ask why is this component of metric tensor constrained by the value of  $-1$ ? In physics, it is reasonable to demand a negative (in the  $---+$  signature), real-valued  $g_{rr}$ , but there is no argument why the interval from  $-1$  to  $0$  should be ruled out. In other words, why should  $u < 0$  be ruled out?

### 5.3. Hidden energy and other kinds of energy

In Sect. 4.3, we already mentioned that there can always be found such a distance  $r_z$  inside the RCO body, where the auxiliary metric function  $u$  equals zero. In an attempt to represent terms  $c^4 u_{out}/G$  and  $-c^4 u_{in}/G$  in the result of the energy calculation (45), we can divide the integration in this relation to two integrations (deLyra, 2023),

$$W_h = \frac{c^4}{G} \int_{R_{in}}^{r_z} \frac{du}{dr} dr = \frac{c^4 u_z}{G} - \frac{c^4 u_{in}}{G} \quad (46)$$

and

$$W_{out} = \frac{c^4}{G} \int_{r_z}^{R_{out}} \frac{du}{dr} dr = \frac{c^4 u_{out}}{G} - \frac{c^4 u_z}{G}. \quad (47)$$

Since  $u_z \equiv u(r_z) = 0$ ,  $u_{in} < 0$ , and  $u_{out} > 0$ , these relations reduce to

$$W_h = -\frac{c^4 u_{in}}{G} = \left| \frac{c^4 u_{in}}{G} \right|, \quad (48)$$

$$W_{out} = \frac{c^4 u_{out}}{G} = \left| \frac{c^4 u_{out}}{G} \right|. \quad (49)$$

The acceleration above the outer RCO surface is proportional to  $u_{out}$  which corresponds to the Newtonian mass  $M_{out}$  according to relation (42). If we observationally determine the mass of RCO, i.e. the mass of a neutron star or a super-massive object in the center of a galaxy or a quasar, then we determine

the Newtonian mass  $M_{out}$  corresponding to  $u_{out}$  which yields the corresponding energy content  $W_{out}$  according to relation (49). The whole energy content is, however, the sum  $W_h + W_{out}$ . Hereafter we refer to energy  $W_h$  as the “hidden energy” and to energy  $W_{out}$  as the “outer-region energy”. In the Newtonian physics, we have only a single concept of energy. The “energy” and “rest energy” are not distinguished. At the same time, there is no hidden energy. The hidden energy is another kind of energy, which should be recognized in GR.

In GR, there has been sometimes considered the “mass within the sphere of radius  $r$ ”. This kind of mass should be abolished. In the context of our analysis, it seems reasonable to consider only a “mass between the spheres of radii  $r_z$  and  $r$ ”.

We note that the hidden energy is significant only in the truly relativistic objects, which cause a significant curving of space-time. In the non-relativistic objects, GR alone (without any postulate) implies  $R_{in} \rightarrow 0$  and, consequently,  $W_h \rightarrow 0$ . One can illustrate this fact by the model of the Sun, which is not very relativistic object. Here, we present only a simple model constructed by using of the equation of state, which is a combination of the polytrope and the equation state of radiation - see relations (20) and (22). We considered the polytrope to be index equal to 3.

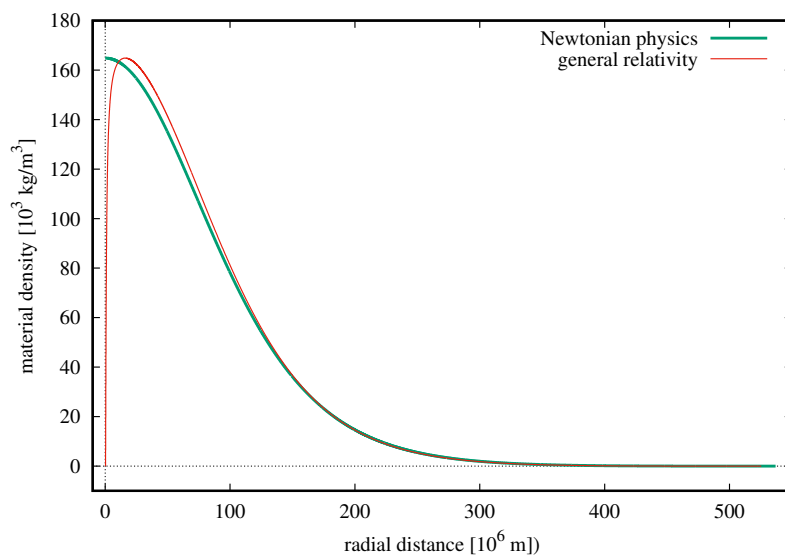


**Figure 5.** The behavior of the material density,  $\rho(r)$ , in the Sun’s interior according to its polytrope model described in Sect. 5.3 (the red curve). The corresponding behavior in the model constructed by using the Newton gravitational law is also shown (the green curve).



To obtain the minimum energy configuration of the solar body (the minimum energy configuration of RCO is discussed more in Sect. 5.4), we construct a series of models by varying the zero-gravity distance,  $r_o$ . Further, the mass of the object in the model must be equal to  $1 M_\odot$ . To achieve this mass, we considered the fixed maximum temperature and varied the maximum pressure (both quantities reach their maximum at the distance  $r_o$ ). Other possibility is to fix the maximum pressure and vary the maximum temperature. However, it appears that the resulting model is almost the same in both cases. The maximum temperature and pressure as well as the chemical composition of the Sun were taken from the standard solar model by [Turck-Chieze et al. \(1988\)](#) (their reference model).

The behavior of the material density inside the Sun's model is shown in Fig. 5 (the red curve). For the sake of a comparison, the polytrope model of the Sun constructed by the Newton gravitational law is also shown (the green curve). We can see that the models are identical in a prevailing volume of the solar body. A difference occurs in a very small volume, in the central region. Specifically,  $R_{in} \sim 10^{-4}$  m (but density,  $\rho$  equals  $10^{-5} \rho_{max}$  already in  $r = 218$  km),  $r_o = 1.6 \cdot 10^4$  km, and  $R_{out} = 5.239 \cdot 10^5$  km. The hidden mass ( $W_h/c^2$ ) equals only  $0.0014 M_\odot$ .

#### 5.4. Minimum energy configuration of RCO

If an RCO possesses not only an outer surface, but an inner surface and a non-zero zero-gravity distance as well, then there is one more degree of freedom. It is, thus, reasonable to ask what a configuration will be acquired. For a set of particles constituting a given RCO, it will obviously be the configuration at which the object has the minimum energy.

Assuming that an RCO consists of  $\eta$  neutrons, its rest mass equals  $M_o = \eta m_n$  regardless the configuration acquired. So, let us construct a series of models for the RCO with the rest mass equal to  $M_o = 5 M_\odot$ , for example. No relation between the Fermi impulse in a starting point of numerical integration and the rest mass of the RCO is known. The required rest mass can be achieved via an iteration, when we vary the input value of the impulse in the starting point. The individual models in the series differ by their zero-gravity distance,  $r_o$ . When this distance is given, then the inner and outer radii of RCO are yielded by modeling.

Having the series of the models, we can investigate the dependence of the RCO's total energy on the zero-gravity distance ([Neslušan, 2019](#)). The dependence is shown in Fig. 6 in our example. Actually, there is a model of RCO with the minimum energy, for  $r_o \doteq 25$  km. So, the object will tend to acquire the configuration with this value of  $r_o$ . The RCOs with  $M < M_o$  (those below the cyan horizontal line in Fig. 6) obey the binding energy condition for a stable configuration (see Sect. 6.1), the minimum energy configuration including.

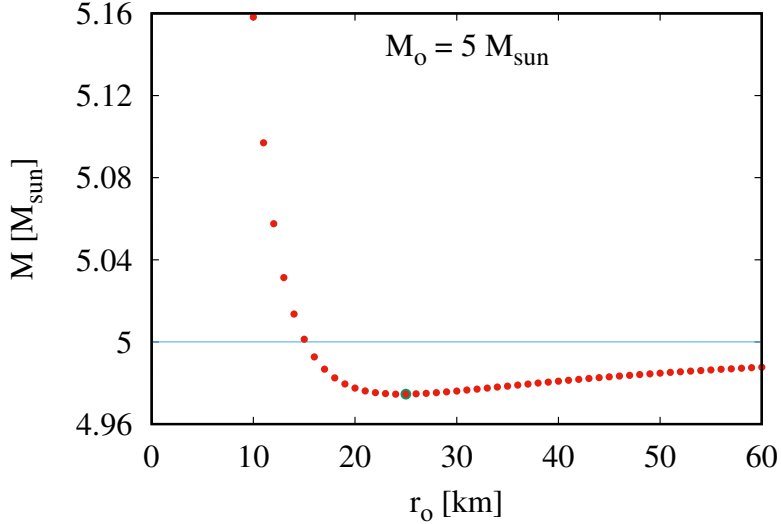


**Figure 6.** The dependence of total energy,  $W$ , in term of mass,  $M = W/c^2$ , on the zero-gravity distance,  $r_o$ , for a series of RCO models, all with the rest mass  $M_o = 5 M_\odot$ . The RCO with the minimum total energy is shown with the green circle (around the red full circle). The zero-gravity distance of this RCO is  $r_o = 25$  km. The cyan horizontal line separates the solutions obeying the binding-energy condition of stability (below the line) from those being in the unstable equilibrium configuration (above the line).

On the contrary, the objects with  $M > M_o$  are in an unstable equilibrium configuration. Since the total energy decreases with the increasing  $r_o$  in the region of instability, these objects should expand after a perturbation occurs. We constructed the  $M = M(r_o)$  dependence for many values of the rest mass; except for the example for  $M_o = 5 M_\odot$  presented here, five other examples were presented in our previous paper (see Fig. 5 in Neslušan, 2019). The minimum of the function  $M = M(r_o)$  always occurred in the region of the stable-equilibrium configuration.

In Fig. 6, we can observe a steep increase of the energy when  $r_o \rightarrow 0$ . It means that the fulfilled-sphere configuration is highly unstable.

The dependence of the outer radius,  $R_{out}$ , on the zero-gravity distance,  $r_o$ , for various configurations of RCO with the same rest mass in the context of the RCO's event horizon is shown in Fig. 7. (In the figure, the example of RCO with the rest mass of  $5 M_\odot$  is presented.) We can see that the outer radius approaches the gravitational radius (the purple curve) when the zero-gravity distance decreases to small values (in the small window showing the detail, the purple curve seems to approach, asymptotically, the blue one). However, when

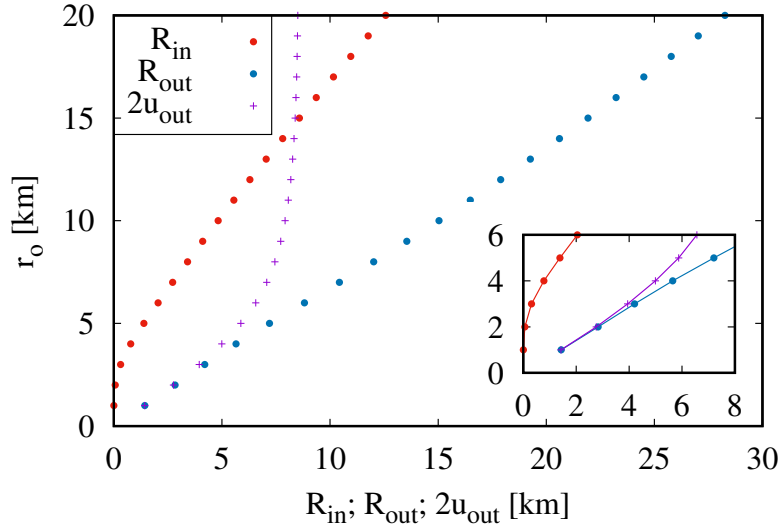


**Figure 7.** The extent of the RCO with the rest mass  $M_o = 5 M_\odot$ , from the inner radius,  $R_{in}$  (red circles), to the outer radius,  $R_{out}$  (blue circles). This extent in the horizontal axis is shown in the dependence on the zero-gravity distance,  $r_o$ , on the vertical axis. (The distance between two, red and blue, points at the same horizontal level is the extent.) The behavior of the gravitational radius,  $2u_{out}$ , as the function of  $r_o$  for the  $5 M_\odot$ -RCO is shown with the purple crosses. In the small window showing a detail at the smallest radii and  $r_o$ , the points resulting from the discrete models are connected with the curve of the corresponding color to demonstrate the approach of the outer radius to the gravitational radius when  $r_o \rightarrow 0$ .

$r_o \rightarrow 0$  then the energy of the object increases as seen in Fig. 6. This fact is even more transparent in Fig. 8 showing the dependence of the difference between the outer RCO radius and the radius of the event horizon on the total energy of the object. We see that the outer radius decreases to reach the event horizon with the increasing energy. In other words, the dependence indicates that a collapse of the object to a black hole requires the delivery of a huge, possibly infinite, amount of energy.

Unfortunately, no analytical, even an analytical static, general solution of the EFEs describing a realistic RCO is known (except for the solution for a photon sphere; see Sect. 7.3), therefore it is impossible to answer the question whether the energy required for a collapse is finite or infinite. At the moment, we have only the indication that some energy is needed. The definitive conclusion on the required energy could be drawn if we knew the analytical solution (the dynamical case) of the EFEs describing the collapse.

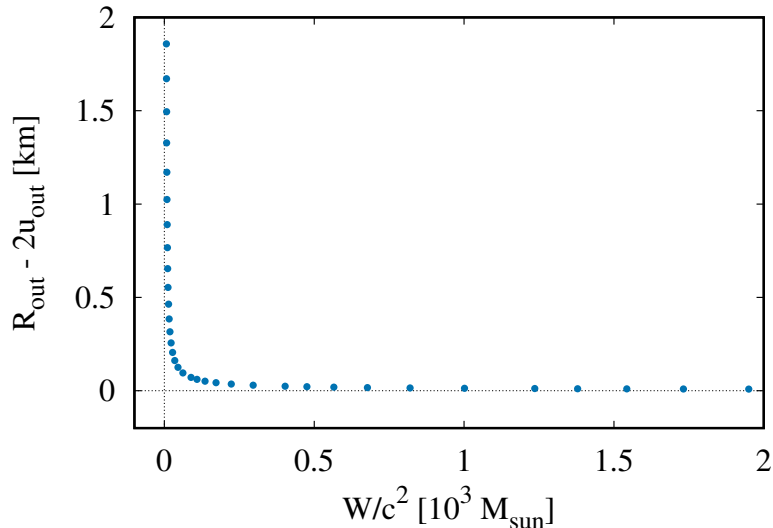


**Figure 8.** The dependence of the difference between the outer radius of a neutron star,  $R_{out}$  and radius of its event horizon, equal to  $2u_{out}$ , on the total energy,  $W$ , given in terms of the corresponding mass,  $M = W/c^2$ . Here, the example of the star with the rest mass  $M_o = 5 M_\odot$  is considered; the blue circles correspond to the individual models of RCO with this rest mass.

### 5.5. On the maximum mass of RCO

In their pioneering work, [Oppenheimer & Volkoff \(1939\)](#) concluded that the mass of a stable neutron star cannot exceed a certain limit. Today, this limit is known as the Oppenheimer-Volkoff upper-mass limit. We know that these authors considered the objects in the shape of the fulfilled sphere. In this section, let us investigate if there is also a constraint on the mass of RCO in the shape of a hollow-sphere.

In [Fig. 9](#), there is shown the dependence of RCO mass on the maximum (in  $r_o$ ) Fermi impulse,  $p_F$ , for several values of the zero-gravity distance. In panel (a) of the figure, the black solid curve shows the dependence for  $r_o = 100$  m. The analogous curves for a smaller value of  $r_o$  could not be distinguished in the resolution of the figure, in the interval of reasonable values of  $p_F$  ( $\sim 0.1$  to  $\sim 2m_n c$ ), from the black curve for  $r_o = 100$  m. The behavior is practically the same for any value of  $r_o < 100$  m, also for  $r_o \rightarrow 0$ . Hence, the black curve shown in [Fig. 9a](#) corresponds to the curve published by [Oppenheimer & Volkoff \(1939\)](#) in their [Figure 1](#). (These authors plotted the dependence of mass on a quantity that corresponded with the maximum Fermi impulse by a complicated, unclear, way. They presented only the part of the curve comprehending the

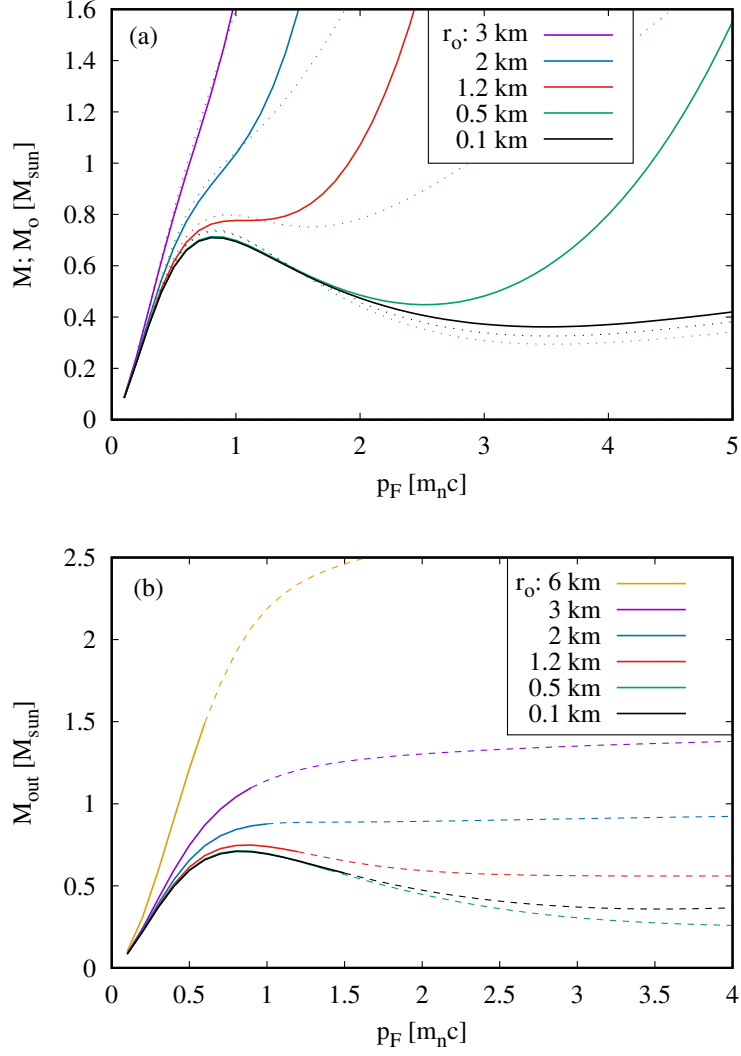


**Figure 9.** The dependence of the RCO mass,  $M$ , and the rest mass,  $M_o$ , on the maximum Fermi impulse,  $p_F$ , for several values of the RCO's zero-gravity distance,  $r_o$  (panel a). The thick solid curve of a given color shows the dependence of the mass and the dotted curve of the same color shows the dependence of the rest mass for the given  $r_o$ . In the intervals of  $p_F$  with  $M_o > M$  (the dotted curve is above the corresponding solid curve), the RCO is in the stable-equilibrium configuration. In panel (b), there is the corresponding dependence of Newtonian mass  $M_{\text{out}}$  on  $p_F$ . The intervals of  $p_F$  where the RCOs are in the stable-equilibrium configuration are shown with a solid curve, the unstable-equilibrium RCO configurations are shown with a dashed curve.

models with a relatively small maximum Fermi impulse.) As seen, the curve has a local maximum at  $p_F \approx 0.8 m_n c$ . This fact has been the main argument for an existence of the upper-mass limit of neutron stars.

The green solid curve in Fig. 9a shows the dependence for  $r_o = 500$  m. In the interval of  $p_F$  from a very small value (we created the models starting with  $p_F = 0.1 m_n c$ ) to  $\sim 2 m_n c$ , it is situated only slightly above the black curve for  $r_o = 100$  m, since there is no significant difference in the behavior for a small  $r_o$  as we mentioned. All curves for a small  $r_o$  have a local maximum, at  $p_F \approx 0.8 m_n c$  or a slightly larger value of  $p_F$ . However, if the dependence is constructed for  $r_o \doteq 1.2$  km (the red solid curve), then there is no maximum; only an inflection point at  $p_F \approx 1.1 m_n c$ . If  $r_o > 1.2$  km, then the mass permanently increases with increasing  $p_F$  (the cyan curve for  $r_o = 2$  km and the purple one for  $r_o = 3$  km in the examples shown in Fig. 9a).

The real objects must be in the stable equilibrium configuration, i.e.  $M < M_o$  according to the binding energy condition of stability (Sect. 6.1). In Fig. 9a, the dependence of the rest mass,  $M_o$ , on the maximum Fermi impulse,  $p_F$ , is shown with a dotted curve of the same color as the dependence  $M = M(p_F)$  for a given  $r_o$ . The intervals of the stable equilibrium RCO configuration are those where the dotted curve is above the solid curve of a given color. We can see that the intervals of the stability range from a small  $p_F$  beyond the local maximum or beyond the point of smallest derivative in respect to  $p_F$  of each curve.

Let us now deal, again, with the modeled RCOs with  $r_o < 1.2$  km. If we consider only the part of the dependence of mass on the maximum impulse, which is terminated before the curve reaches its local minimum (as [Oppenheimer & Volkoff \(1939\)](#) did), it seems that the previous maximum, at  $p_F \approx 0.8 m_n c$ , is the absolute maximum. However, as shown in Fig. 9a, a continuation of the dependence to large values of  $p_F$  reveals that there is a local minimum (at  $p_F \approx 3.5 m_n c$  in the case of  $r_o = 100$  m and at  $p_F \approx 2.5 m_n c$  when  $r_o = 500$  m) and mass again increases for a larger  $p_F$ -values. Of course, the behavior of the  $M = M(p_F)$  dependence in the region of extreme values of  $p_F$  is irrelevant to real objects because of two reasons. First, the RCOs would be in an unstable equilibrium configuration (the black dotted or green dotted curves are below the black solid or green solid curve, respectively). Second, the extreme impulse  $p_F$  implies such a huge energy of neutrons that we can expect transmutations of the particles and, consequently, the considered EoS would no longer be valid. Hence, the continuation of the  $M = M(p_F)$  dependence is interesting only from the point of view of mathematics.

If we deal with the RCOs in the shape of a hollow sphere, the mass corresponding to the outer-region energy is the quantity we measure in observations, as we already mentioned at the end of Sect. 4.3. The dependence of the measured outer-region - or Newtonian - mass,  $M_{out}$ , on the maximum Fermi impulse is shown in Fig. 9b, again for several values of  $r_o$ . The part of the dependence in the region of stable equilibrium is shown with a solid line (a continuation to

the region of the unstable equilibrium is shown with a dashed line). One can see that the maximum  $M_{out}$  in the regions of stability increases with increasing  $r_o$ .

When one constructs the dependence  $M_{out} = M_{out}(p_F)$  for a large enough value of  $r_o$ , there is an indication that  $M_{out}$  (the measured “mass”) can, most probably, increase up to an arbitrarily large value. Without an analytical solution, we cannot prove if an increase above all limits is actually possible. Anyway, even if there is a maximum value of  $M_{out}$ , this value is, obviously, much larger for the hollow-sphere than the fulfilled-sphere RCO. In Fig. 9b, the maximum  $M_{out}$  of the stable RCO with  $r_o = 6$  km (the orange solid curve) is  $1.49 M_\odot$ . If we search for the maximum in the series of RCO models for a larger  $r_o$ , for  $r_o = 10, 15, 20, \text{ or } 25$  km for example (these results are not shown in Fig. 9b because of its better transparency), then the maximum  $M_{out}$  of RCO in the stable-equilibrium configuration  $M_{out} = 2.14, 2.62, 3.18, \text{ or } 3.39 M_\odot$ , respectively.

## 6. Condition of hollow-sphere-RCO stability and other conditions

### 6.1. Binding-energy criterion of RCO stability

EFEs (2)–(5) or those in form (9), (10), and (16) give a static solution for a RCO, therefore every RCO described by a solution of these equations must be in a balanced configuration. However, the RCO equilibrium can be stable or unstable. We are, of course, interested in the models of RCO in the stable equilibrium configuration. An RCO is in the stable equilibrium, if its binding energy is positive (Tooper, 1965), i.e.

$$W_{b.e.} = W_o - W > 0. \quad (50)$$

In the example of a neutron star presented in Sect. 4, the binding energy condition is obeyed because  $Mc^2 < M_o c^2$  ( $M = 4.97457 M_\odot$  and  $M_o = 5.00000 M_\odot$ ). We remind that  $W_o$  and  $W$  are the rest energy and total energy of RCO, respectively. The rest energy is

$$\begin{aligned} W_o = M_o c^2 &= 4\pi \bar{m} \int_{R_{in}}^{R_{out}} n r^2 e^{\lambda/2} dr = \\ &= 4\pi \int_{R_{in}}^{R_{out}} \frac{\rho r^2}{\sqrt{1 - \frac{2u}{r}}} dr. \end{aligned} \quad (51)$$

The symbol  $\bar{m}$  stands for the mean mass and  $n$  is the number density of the RCO-constituting particles.

When condition (50) is applied, it is implicitly assumed that the generation of thermal energy in nuclear reactions is negligible, i.e.  $W_o$  is constant, and also the energy of radiation is negligible. However, the energy of radiation is

sometimes a significant or dominant type of energy, so far, therefore we have to modify the condition for the stable equilibrium given by inequality (50).

The modification is necessary, since the energy of the radiation of a RCO in thermal equilibrium cannot be converted into the kinetic type energy of gas particles; there is no contribution of energy from the radiation helping these particles to overcome the RCO's potential barrier. The radiation tends to be in the thermodynamic equilibrium with the gas (plasma). Some radiation energy could be delivered to the gas (causing an increase of its energy and, hence, temperature) only if the temperature of radiation decreased, but this would contradict the second law of thermodynamics. Therefore, when the energy of radiation is significant, the binding energy should be calculated as

$$W_{b.e.} = W_o - W_g, \quad (52)$$

where  $W_g = W - W_r$  is the total energy reduced by the energy of radiation,  $W_r$ .

We note that Tooper's binding-energy criterion for stability was abandoned in the works published in the last decades. The stability has been mostly evaluated performing the perturbation analyses. The reason of why the binding-energy criterion was abandoned has never been given, however. The condition (50) or (52) should be the primary condition of stability. If it is not obeyed, the object cannot be stable. Namely, if there is enough energy to overcome the gravitational potential of an object, the object must expand. We can compare this to the celestial-mechanics problem of two bodies the integral of their energy is positive. Then, we cannot say that one object remains in a bound, elliptical, orbit around the other. It must move in the unbound, hyperbolic, orbit.

## 6.2. Other conditions to describe a real object

To create a model relevant to a realistic RCO, several conditions in addition to the binding-energy condition were published by various authors. In this section, we discuss some of these conditions, as summarized by Ivanov (2017) and recently discussed by Hernández et al. (2021). Some of the conditions are, however, relevant only to the RCO in the shape of the fulfilled sphere, therefore we omit them in this section, but are discussed in Sects. 4.4, 4.5, and 7.

Except for the demand on the positive binding energy, the following conditions for an isotropic RCO should be mentioned.

(1) Components of the metric tensor,  $e^\lambda$  and  $e^\nu$ , are positive, finite, and free from any singularity within the matter distribution.

(2) At the surfaces of the RCO, the RCO-body solution for the components of the metric tensor should match continuously their counterparts in the OSM. In other words, the components of the RCO-body metric tensor and their derivatives in respect to  $r$  should equal to the corresponding components and their derivatives in the OSM at both RCO surfaces. In the case of the spherically symmetric RCO, having non-zero only the diagonal components of the



metric tensor, the spatial transversal components,  $g_{\theta\theta}$  and  $g_{\varphi\varphi}$ , are identical in the RCO-body metrics and OSM, therefore their matching is obvious. There is also the match of the  $g_{rr}$  component and its derivative due to the intrinsic consistency of GR.

However, the  $g_{tt}$  component is not present in the EFEs; there is only the derivative of the auxiliary function  $\nu$ . Hence,  $g_{tt}$  is not uniquely determined by the EFEs and its tailoring deserves an attention. The fact that the derivative  $d\nu/dr$  can be found solving the EFEs means that the behavior of  $\nu$ , as a function of the distance  $r$ , is given, but there is an unknown integration constant,  $\nu_K$ , which can be added to the function  $\nu = \nu(r)$  at every  $r$ .

The value of the constant  $\nu_K$  suitable for the tailoring can be found either in an iteration or in the following way. We start the numerical integration with an arbitrary initial value,  $\nu_a$ , of the function  $\nu$  and perform the integration to the outer radius,  $R_{out}$ . The integration yields a value of  $\nu$ , which we denote  $\nu_{Ra}$ , at  $R_{out}$ . At the same time, the integration yields the value,  $u_{out}$ , of the function  $u$  at  $R_{out}$ , therefore we can calculate the relevant  $g_{tt}$  component in the OSM in  $R_{out}$ :  $g_{tt}(R_{out}) = 1 - 2u_{out}/R_{out}$ . The corresponding  $\nu$  equals  $\nu_{OSM} = \ln(1 - 2u_{out}/R_{out})$ . Obviously, constant  $\nu_K = \nu_{OSM} - \nu_{Ra}$ . The initial value of  $\nu$  suitable for the tailoring, which we denote by  $\nu_b$ , is equal to  $\nu_a + \nu_K$ , explicitly

$$\nu_b = \nu_a + \ln\left(1 - \frac{2u_{out}}{R_{out}}\right) - \nu_{Ra}. \quad (53)$$

We implicitly assumed the calibration  $K_{\nu,o} = 1$  in the calculation of  $\nu_b$ . If the integration is repeated, whereby  $\nu_b$  is used as the input, it yields the behavior of  $g_{tt}$  which can be tailored to its OSM counterpart at  $R_{out}$ .

(3) The pressure should vanish at the surfaces, except for radiation pressure. (We consider the isotropic solution, therefore we do not distinguish between the radial and tangential components of the pressure.) We require, in addition, the material density should vanish at the RCO surfaces.

(4) The energy density and pressure should be positive inside the RCO body. For the energy density this demand coincides with the null energy condition. If both pressure and energy density are positive in the RCO's body, then all energy conditions, except for the dominant and strong (see the next item), are obeyed.

(5) The dominant energy condition should be satisfied, i.e.  $E \geq P$ , anywhere inside the RCO body. It is desirable that even the strong energy condition is satisfied. This condition requires  $E \geq 3P$ .

(6) The causality condition should be satisfied. It says that the speed of sound should not surpass the speed of light, or  $0 < dP/dE \leq 1$ .

(7) The adiabatic index,  $\Gamma = [(E + P)/P]dP/dE$ , which is the ratio of two specific heats, should be  $\Gamma \geq 4/3$ .

(8) The distribution of mass obeys the principle of minimum action. The total energy of RCO is minimal possible energy for the set of particles of gas

constituting the object.

We found that, for a reasonable EoS, all these conditions are obeyed for a large variety of RCOs. Condition (1) is satisfied for every real-values  $\lambda$  and  $\nu$  and these quantities are real-valued if all components of the metric tensor are real. For several EoSs we also proved that the behavior of all quantities in the RCO body is continuous, without any singularity. As well, it is possible to prove, for the specific EoSs, that there are always the inner and outer surfaces in which the material density vanishes and the OSM can be smoothly tailored to the metrics of the RCO-body.

If the EoS for radiation or a polytrope with radiation is considered, then the energy density and pressure are non-zero down to the exact center of the object and up to the infinite distance from it. However, even in the case of a radiation sphere, there is a steep decrease of the pressure and energy density in two finite object-centric distances. The first can be regarded as inner and the second as the outer physical surface. Below the inner and above the outer surface the metrics can be well approximated with the OSM (an example can be found in (Neslušan, 2017b) or (Neslušan, 2017a)). Thus, conditions (2) and (3) are obeyed, practically.

The reasonable EoS, i.e. the EoS to describe a real object, contains only the positive energy density and pressure, therefore the obeying of condition (4) is obvious. For the EoS given by relations (13)–(15), we can show that

$$E = 3P + \frac{m_n^4 c^5}{4\pi^2 \hbar^3} \sum_{j=1}^{\infty} \frac{1}{(2j+1)!} \left(\frac{\tau}{2}\right)^{2j+1}. \quad (54)$$

Hence,  $E \geq 3P$  for  $\tau \geq 0$ , which is always the case. Therefore, condition (5), i.e. the dominant as well as strong energy conditions, are obeyed. The conditions are also obeyed for the EoS of radiation,  $E = 3P$ , and EoS in the form of a polytrope (relations (19) and (20)) when the polytrope index  $N \geq 1$  (the dominant energy condition) or  $N \geq 3$  (both dominant and strong energy conditions).

Causality condition (6) is also obeyed for all the three above mentioned EoSs. For EoS (14) and (15), we can show that

$$\frac{dP}{dE} = \frac{1 \cosh \frac{\tau}{2} - 1}{3 \cosh \frac{\tau}{2} + 1}. \quad (55)$$

For any positive  $\tau$ , it is therefore valid  $dP/dE > 0$  and  $dP/dE$  approaches  $1/3$  when  $\tau$  acquires large values. When  $\tau \rightarrow 0$ , then  $dP/dE \rightarrow 0$ . If  $E = 3P$ , then  $dP/dE = 1/3$ . For the polytrope, one can find

$$\frac{dP}{dE} = \frac{1}{N} \frac{(N+1)K_P \rho^{1/N}}{(N+1)K_P \rho^{1/N} + c^2}, \quad (56)$$

therefore  $dP/dE < 1$  for  $\rho > 0$  if  $N \geq 1$ .

In the case of EoS (14) and (15), the adiabatic index,  $\Gamma$ , is larger than  $4/3$  and condition (7) is obeyed for large values of the Fermi impulse,  $p_F$ , and approaches  $4/3$  when  $p_F$  decreases to zero. If the EoS is  $E = 3P$ , then  $\Gamma = 4/3$ . For the polytrope,  $\Gamma = 1 + 1/N$ , therefore condition (7) is obeyed for  $N \leq 3$ .

Concerning condition (8), we found that it can be obeyed (there is a minimum of the function  $M = M(r_o)$ ) for the EoS of the cool, degenerated, Fermi-Dirac gas characterized with relations (14) and (15). We further found that it is also obeyed for polytrope (19) and (20), as well as the EoS which is the combination of the polytrope and EoS for radiation,  $E = 3P$ . On the contrary, no minimum of the function  $M = M(r_o)$  was found for the EoS of the degenerated ion-electron gas, i.e. for the gas constituting the white-dwarf stars.

## 7. A confrontation of two concepts of RCO

In this section, we discuss the traditional fulfilled-sphere concept versus the new hollow-sphere concept of RCO.

### 7.1. On the requirement of the regularity of metrics

When a relativistic star or other object generating a strong gravity is modeled, it is demanded, among other things, that the metrics should be regular at the origin. The demand of regularity was specified by, e.g., Misner et al. (2017) (in their paragraph 23.5) who calculated the mass inside the radius  $r$ ,

$$M_r(r) = \int_0^r 4\pi r^2 E dr + M_r(0), \quad (57)$$

and argued that the constant of integration  $M_r(0)$  must be zero. The first problem with Eq.(57) is the lower limit of the integration. It has always been assumed to be zero, but the question why it is zero has never been answered. This question is non-trivial in the GR. The zero lower limit means that the distribution of matter in the RCO is implicitly assumed to extend to its proper center. However, it means that the distribution is *assumed*, not proved.

According to the authors requiring the regularity of the metrics at the origin, the demand  $M_r(0) = 0$ , implying a space geometry that is smooth at the origin, is physically acceptable in contrast to a non-zero value, which means a geometry with a singularity at the origin and is physically unacceptable.

However, can the demanded equality  $M_r(0) = 0$  be achieved within GR? This demand has never been proved to be possible. On the contrary, the equation of geodesic implies the relativistic term of the gravitational acceleration, which cannot be zero for an RCO of a non-zero mass and which implies that the outer layers of the RCO attract the layers below them outward from the RCO center. It is possible (although this has been proved neither) that there is always a finite RCO-centric distance, below which the net gravity of the outer layers

dominates over the downward oriented gravitational action of lower layers. Thus, there should necessarily occur, at the RCO consisting of a compressible fluid, an inner physical surface and the function  $M(r)$  is zero at a finite object-centric distance. The demand  $M_r(0) = 0$  can, paradoxically, be surely obeyed only after GR is ignored at a region around the RCO center.

The matter inside the RCO could be distributed down to its center, if we completed the demand  $M_r(0) = 0$  with another demand that every RCO must consist either of an incompressible fluid or a solid material. In the case of solid material, the stress-energy tensor (7) is irrelevant and no else stress-energy tensor was considered. The demand of incomprehensibility would also be problematic, especially for the super-massive RCOs. Penrose (1969) pointed out that the mean density of an RCO decreases with its mass. An estimate of the mean density can be done in the following way.

Let us define the ‘‘compactness’’ of RCO,  $\zeta$ , as the ratio of the gravitational Schwarzschild and outer-surface radii, i.e.  $\zeta = R_g/R_{out}$ . The mean density,  $\langle\rho\rangle$ , of the fulfilled-sphere RCO with the mass  $M$  equals  $\langle\rho\rangle = 3M/(4\pi R_{out}^3)$ . Let us consider two RCOs with masses  $M_1$  and  $M_2$ , which have the same compactness, i.e. there is valid  $R_{g1}/R_{out1} = R_{g2}/R_{out2}$ . From the latter,

$$R_{out2} = \frac{M_2 R_{out1}}{M_1}. \quad (58)$$

If one calculates the ratio of mean densities of both aforementioned RCOs, he or she obtains

$$\frac{\langle\rho\rangle_2}{\langle\rho\rangle_1} = \frac{3M_2}{4\pi R_{out2}^3} \left( \frac{3M_1}{4\pi R_{out1}^3} \right)^{-1} = \frac{M_2}{M_1} \left( \frac{R_{out1}}{R_{out2}} \right)^3. \quad (59)$$

When the outer radius of the second RCO,  $R_{out2}$ , is expressed by relation (58), the ratio of the mean densities equals

$$\frac{\langle\rho\rangle_2}{\langle\rho\rangle_1} = \frac{M_1^2}{M_2^2}. \quad (60)$$

It means, the mean density of RCO, being in the form of a fulfilled sphere, is reciprocally proportional to its mass squared. For example, if the mean density of a neutron star having the mass of order of  $10^0 M_\odot$  is  $\sim 10^{17} \text{ kg m}^{-3}$ , then the mean density of a super-massive RCO with the mass of order of magnitude  $10^9 M_\odot$  is 18 orders of magnitude smaller than the mean density of the neutron star, i.e. it equals about  $10^{-1} \text{ kg m}^{-3}$ . It is even smaller than the density of the Earth’s atmosphere at the Earth’s surface. This indicates that the regions of RCO with a relative small material density rather consist of a common gas than an incomprehensible matter or solid matter.

Misner et al. (2017) were right that there is a singularity at  $r = 0$  if  $M(0) \neq 0$ . However, this singularity does not seem to be problematic as we argued in

Sect. 4.5. It is of the Big-Bang type and, therefore, an acceptable singularity and, until it exists, it cannot be visited, in principle, by any particle or object (observer). It can thus be regarded as a point of space-time not belonging to our universe.

### 7.2. One or two degrees of freedom?

When one demands the distribution of RCO matter down to its center, he or she arbitrarily cancels one degree of freedom. While the hollow-sphere RCO can acquire (i) a various zero-gravity distance,  $r_o$ , and (ii) a various thickness, i.e. difference  $R_{out} - R_{in}$ , the fulfilled-sphere RCO can have only various outer radius. From the point of view of GR, it is not clear what keeps the matter of the fulfilled-sphere RCO distributed down to its center. If one wants to create a model of the fulfilled-sphere RCO, he or she must ignore the second, relativistic, term of acceleration (29) when they determine the action of upper material layers onto the lower layers. It means that the relativistic acceleration is replaced in this case by its Newtonian counterpart, in fact. In the past, this replacement has escaped the experts' attention, since it has always been assumed implicitly. Or, the researchers kept in their minds the postulate of the Minkowski metrics inside the spherical shell.

When the stability of fulfilled-sphere neutron stars was proved via various perturbation analyses, it was likely just the ignorance of the relativistic term of acceleration causing a positive result. If the second degree of freedom is taken into account, then the fulfilled-sphere RCO (or RCO with a very small  $r_o$ ) is highly unstable according to the binding-energy criterion.

### 7.3. Does a solution for the fulfilled-sphere RCO exist?

The question in the title of this sub-section could be answered if the analytical solutions of the EFE for the realistic EoS were known. Then, the problem of a fulfilled-sphere versus hollow-sphere concept of RCO could be solved. Unfortunately, an analytical solution of the EFEs is known only for one realistic EoS, the EoS of radiation  $E = 3P$ , i.e. a photon sphere.<sup>2</sup> If one considers, for example, the polytrope or the mixture of polytrope and radiation, one has to use numerical methods (Stephani et al., 2009, p. 250). In the following, we describe an indication of the answer at least in the case of the photon sphere.

For the EoS of  $E = 3P$ , the analytical solution was found by Hajj-Boutros (1989) in the form of the elliptic integral of the first kind. To reveal whether the solution for the RCO in the form of a fulfilled sphere exists, we however need only some simpler relations, which occurred as an intermediate result in Hajj-Boutros' derivation.

---

<sup>2</sup>We speak here about the realistic EoS in sense that this equation gives the relation between the pressure and energy density of a real entity (radiation).

In his work, the author used the isotropic coordinates with the auxiliary metric functions  $\mu = \mu(r)$  and  $\nu = \nu(r)$ . The line element in these coordinates is defined as

$$ds^2 = -e^\mu(dr^2 + r^2 d\vartheta^2 + r^2 \sin^2 \vartheta d\varphi^2) + e^\nu c^2 dt^2 \quad (61)$$

and the analogs of EFEs (2), (3), and (5) with the components of the stress-energy tensor given by matrix (7) are

$$\kappa P = e^{-\mu} \left( \frac{\mu'^2}{4} + \frac{\mu'\nu'}{2} + \frac{\mu' + \nu'}{r} \right), \quad (62)$$

$$\kappa P = e^{-\mu} \left( \frac{\mu''}{2} + \frac{\nu''}{2} + \frac{\nu'^2}{4} + \frac{\mu' + \nu'}{2r} \right), \quad (63)$$

$$\kappa E = e^{-\mu} \left( \mu'' + \frac{\mu'^2}{4} + \frac{2\mu'}{r} \right). \quad (64)$$

Eq.(12) remains valid for the isotropic coordinates in the unchanged form.

Hajj-Boutros (1989) suggested to change the variable  $r$ :

$$\xi = \ln r. \quad (65)$$

In agreement with this author, we use a dot (double dot) to denote the derivative (second derivative) in respect to the new variable,  $\xi$ . One easily obtains  $\mu' = e^{-\xi}\dot{\mu}$ ,  $\nu' = e^{-\xi}\dot{\nu}$ ,  $\mu'' = e^{-2\xi}(\ddot{\mu} - \dot{\mu})$ , and  $\nu'' = e^{-2\xi}(\ddot{\nu} - \dot{\nu})$ . Subsequently, Eqs.(62)–(64) can be re-written, for  $E = 3P$ , as

$$S = \frac{1}{4}\dot{\mu}^2 + \frac{1}{2}\dot{\mu}\dot{\nu} + \dot{\mu} + \dot{\nu}, \quad (66)$$

$$S = \frac{1}{2}\ddot{\mu} + \frac{1}{2}\ddot{\nu} + \frac{1}{4}\dot{\nu}^2, \quad (67)$$

$$3S = \ddot{\mu} + \frac{1}{4}\dot{\mu}^2 + \dot{\mu}, \quad (68)$$

where we denoted  $S = \kappa P e^\mu e^{2\xi}$ .

Hajj-Boutros derived relations

$$\dot{\nu}^2 = A \sinh(\nu + \alpha) - 2, \quad (69)$$

$$\mu = -2\xi - \nu - 2 \ln(\dot{\nu}) + C_1, \quad (70)$$

where  $A$ ,  $\alpha$ , and  $C_1$  are the integration constants. The last relation can be re-written as

$$\dot{\nu}^2 = \frac{C_\mu}{r^2} e^{-\mu-\nu}, \quad (71)$$

where  $C_\mu = e^{C_1}$  is another constant. Comparing (69) and (71) and after some algebraic handling, we obtain

$$A \sinh(\nu + \alpha) - 2 = \frac{C_\mu e^{-\mu-\nu}}{r^2}. \quad (72)$$

Eq.(12) can be integrated (Tolman & Ehrenfest, 1930) and we obtain

$$P = P_o e^{-2\nu}, \quad (73)$$

where  $P_o$  is an integration constant corresponding with the maximum pressure. From the latter,  $e^{-\nu} = \sqrt{\frac{P}{P_o}}$ . This relation enables the replacement of the quantity  $\nu$  with pressure,  $P$ , in Eq.(72), i.e.

$$\frac{A}{2} e^\alpha \sqrt{\frac{P_o}{P}} - \frac{A}{2} e^{-\alpha} \sqrt{\frac{P}{P_o}} - 2 = \frac{C_\mu e^{-\mu}}{r^2} \sqrt{\frac{P}{P_o}}. \quad (74)$$

Using notation  $B = e^\alpha \sqrt{P_o}$  and  $C_2 = e^\alpha C_\mu$ , the last equation can be changed to the quadratic equation of the variable  $P$ ,

$$\hat{a}P^2 + \hat{b}P + \hat{c} = 0, \quad (75)$$

with coefficients

$$\hat{a} = (Ar^2 + 2C_2 e^{-\mu})^2, \quad (76)$$

$$\hat{b} = -2B^2 (A^2 r^2 + 8r^2 + 2AC_2 e^{-\mu}) r^2, \quad (77)$$

$$\hat{c} = A^2 B^4 r^4. \quad (78)$$

Now, we can investigate the behavior of the pressure and, at the same time, energy density (since  $E = 3P$ ) in the center of RCO. The regularity of metrics in the center requires that the  $g_{rr}$  component of the metric tensor, which equals  $e^\mu$  in the isotropic coordinates, must acquire a finite value. If  $e^\mu$  is finite then  $\hat{a} \rightarrow 4C_2^2 e^{-2\mu}$ ,  $\hat{b} \rightarrow 0$ , and  $\hat{c} \rightarrow 0$  for  $r \rightarrow 0$  and the roots of Eq.(75) are

$$P|_{1,2} = \frac{-\hat{b} \pm \sqrt{\hat{b}^2 - 4\hat{a}\hat{c}}}{2\hat{a}} \rightarrow 0. \quad (79)$$

Hence, our analysis results in the conclusion that a stable relativistic photon sphere cannot possess a form of the fulfilled sphere; the pressure and energy density in its center are falling to zero.

Of course, we still do not know the behavior of the pressure and energy density in the center of RCO consisting of a gas described with the realistic EoS, as the polytrope, or EoS of the cool, degenerated, Fermi gas, or other, more sophisticated EoS. However, the above-mentioned conclusion indicates that the fulfilled-sphere configuration of RCO is not obvious.

#### 7.4. Remarks about the concept of black hole

At the hollow-sphere RCO, we cannot avoid the singularity in its center. However, we cannot either avoid a singularity at the fulfilled-sphere RCO, those with the mass above the Oppenheimer-Volkoff limit. For a very massive object, we have to accept their collapse and singularity at the event horizon. The experts attempted to demonstrate that the singularity at the distance  $r = R_g$  (i.e. at the event horizon) is just a coordinate artifact. Several coordinate transformations with no singularity in any component of the metric tensor were found and this was used as the argument.

However, GR is based, except of other, on the principle that the line element is invariant under any transformation within this theory. Therefore, if the line element,  $ds$ , in one coordinate system contains a singular point, the line element  $ds'$  in every other (“dashed”) coordinate system must also contain the corresponding singular point. It means that the singularity cannot be removed, in principle.

One can demonstrate the fact that there is always valid that  $ds^2 = ds'^2$  in the case of, e.g., the Kruskal-Szekeres coordinates which are well known to be used in the incorrect proving that  $r = R_g$  is not a genuine singularity. In these coordinates, new variables  $X$  and  $T$  are defined as

$$X = \sqrt{\frac{r}{R_g} - 1} e^{r/(2R_g)} \cosh\left(\frac{ct}{2R_g}\right), \quad (80)$$

$$T = \sqrt{\frac{r}{R_g} - 1} e^{r/(2R_g)} \sinh\left(\frac{ct}{2R_g}\right), \quad (81)$$

in the region above the event horizon. (In the region below the event horizon, variables  $X$  and  $T$  are defined by the similar relations. Considering them, the same conclusion as we draw below can be derived.) The line element squared,  $ds'^2$ , in the new coordinates can be given as

$$ds'^2 = \frac{4R_g^3}{r} e^{-r/R_g} (dX^2 - dT^2) + r^2 d\vartheta^2 + r^2 \sin^2 \vartheta d\varphi^2 \quad (82)$$

(the  $+++-$  signature is used, here). Actually, there is no singular point at any distance  $r > 0$  in forms  $(4R_g^3/r)e^{-r/R_g}$ ,  $r^2$ , or  $r^2 \sin^2 \vartheta$ .

When we, however, calculate the differential  $dX^2 - dT^2$  squared, we obtain

$$\begin{aligned} dX^2 - dT^2 &= \left(\frac{1}{2R_g} e^{r/(2R_g)}\right)^2 \\ &\cdot \left[ \left(\frac{r}{R_g}\right)^2 dr^2 - \left(\frac{r}{R_g} - 1\right) c^2 dt^2 \right]. \end{aligned} \quad (83)$$



We see that  $dX^2 - dT^2 \rightarrow \infty$  and, then,  $ds'^2 \rightarrow \infty$  for  $r \rightarrow R_g$ . The singularity does not disappear in the new (dashed) coordinate system. In addition, the differential of any quantity should acquire an infinitesimally small value. Otherwise, one basic assumption of the differential calculus is violated. It means that the Kruskal-Szekeres coordinates should never be used in the vicinity of  $R_g$ .

The collapse of very massive fulfilled-sphere RCOs below their event horizon was not accepted by some GR experts. It is well known that Einstein and Eddington were reluctant to the concept of a black hole. Concerning this object, Eddington wrote (Chandrasekhar, 1972): *“Chandrasekhar shows that a star of mass greater than a certain limit remains a perfect gas and can never cool down. The star has to go on radiating and radiating and contracting and contracting until, I suppose, it gets down to a few kilometers’ radius when gravity becomes strong enough to hold the radiation and the star can at least find peace. I felt driven to the conclusion that this was almost a reductio ad absurdum of the relativistic degeneracy formula. Various accidents may intervene to save the star, but I want more protection than that. I think that there should be a law of Nature to prevent the star from behaving in this absurd way.”* Our result indicates that Eddington could be right. There actually exists the “law of Nature” which can prevent the star from an infinite collapse. It is the relativistic gravity itself. Deeply inside the compact object, there appears such a position of the mass center of the dominant-gravity matter that the net gravitational attraction becomes oriented outward from the object’s center.

In Sect. 5.4 we stated that we do not know, at the moment, whether the energy needed for the gravitational collapse is finite or infinite. If this energy were finite, then black holes would be possible, although not necessary, a final stage of very massive objects without the internal energy source. If the energy were infinite, the black holes would be energetically forbidden and, thus, impossible as Eddington claimed.

The skepticism concerning the black-hole concept seems to be in a contradiction with the claims of some experts who said the collapse of a very massive object below its event horizon was proved in the papers by Oppenheimer & Volkoff (1939) and Oppenheimer & Snyder (1939). A detailed inspection of the first paper however reveals that Oppenheimer and Volkoff discovered that there is no solution of the EFEs for a stable neutron star with the mass exceeding the upper mass limit. In their era, there existed the models of stars and planets within the Newtonian gravity which was oriented toward the center throughout the whole body of object. It is therefore not very surprising that they assumed a collapse of an unstable object.

In their paper, Oppenheimer and Snyder considered the previous conclusion drawn by Oppenheimer and Volkoff that a massive compact object had necessarily to collapse and, based on this conclusion, they *described* the collapse when the gradient of pressure to resist the gravitational attraction is negligible. Their work cannot be a proof of the collapse since such a proof can only be done when one evaluates both the strength of the gravitational attraction

and oppositely acting gradient of pressure and demonstrates that the gravity is dominant (Neslušan, 2019). But the gradient of pressure was not evaluated by the authors.

It is worth noting that the non-existence of black holes would not be in a disagreement with observations. Murk (2022) studied the observability of the black holes and argued that “identifying the observed astrophysical black hole candidates as genuine black holes is not justified based on the currently available observational data”. Actually, it is necessary to realize that various phenomena, which are today ascribed to the black holes, occur due to a strongly curved space-time in the vicinity of compact objects. However, such the space-time can also be configured by a dark RCO, which is not collapsed below its event horizon.

## 8. Conclusions

In our paper, we demonstrated of how GR works, indeed, in the astrophysics of the RCOs. The particular conclusions follows.

(1) The formula to calculate a gravitational acceleration consists, basically, of two terms, Newtonian and relativistic. The relativistic term represents a repulsive gravity which weakens the attractive Newtonian term in the region of space above the event horizon.

(2) Due to the relativistic term in acceleration, there always occurs an outward oriented gravitational action in the central region of a spherically symmetric distribution of matter.

(3) In the RCOs with their mass smaller than the Oppenheimer-Volkoff mass limit, the volume of the region of the outward oriented gravity can be arbitrarily small. At the moment, we do not know if the volume of the region can be zero. This circumstance enabled to postulate the metrics without a singularity in the center of RCOs and, practically, create the models of RCOs in the form of (an approximate) fulfilled sphere, with the matter distributed down to the RCO center.

(4) The EFEs imply the RCOs, consisting of a compressible perfect fluid, in the form of a hollow sphere. Inside such an RCO, there exists an RCO-centric distance below which the metric quantity  $u$ , related to the  $g_{rr}$  component of the metric tensor, is negative. The corresponding energy is, however, positive. We named this energy as “hidden energy”. This kind of energy never occurs within the Newtonian physics. It was found that its value can be several orders of magnitude larger in the super-massive RCOs than the value of their energy derived from the detectable Newtonian mass, which determines the acceleration of the objects above the RCO’s outer surface.

(5) A model of a traditional, fulfilled-sphere RCO (or a quasi-fulfilled sphere RCO in fact) can be constructed only with a mass smaller than the Oppenheimer-Volkoff upper mass limit. Since no analytical solution of the EFEs exists to de-

scribe a real RCO, it is unknown whether there is or is not a mass limit in the case of hollow-sphere RCOs; if so, then this limit must be considerably larger than the Oppenheimer-Volkoff limit.

(6) When it is postulated that any realistic RCO must be in the form of a fulfilled sphere, then the essential part of the solutions of the EFEs is forbidden. Due to this prohibition, there occurs the Oppenheimer-Volkoff upper mass limit and scientists are forced to establish the concept of a black hole to describe a final stage of more massive objects. Thus, the concept of a black hole is not implied by GR, but it appeared, on the contrary, due to the prohibition of the large, essential, part of this theory.

(7) To construct a model of RCO in the form of a fulfilled sphere, one must cancel one degree of freedom; only the RCO outer radius is variable in this case. He or she must, usually implicitly, assume a fictitious force keeping the distribution of RCO matter down to its center. The hollow-sphere RCO consisting of a given set of constituting particles can have a various zero-gravity distance and thickness; thus, there are two degrees of freedom.

(8) The stable-equilibrium configuration of a hollow-sphere RCO consisting of a given set of constituting particles occurs for a zero-gravity distance, which is significantly larger than zero. If this distance decreases, the RCO's total energy increases. If the zero-gravity distance is smaller than a certain limit, the object is in an unstable-equilibrium configuration. If the zero-gravity distances approaches zero, i.e. the hollow-sphere RCO is going to become the fulfilled-sphere object, its energy is tremendous (possibly approaching infinity) and its stability is very problematic.

(9) There is no singularity in the center of the fulfilled-sphere RCO. However, this smoothness of metrics is only postulated, at the moment. No solution of the EFEs for a realistic EoS implying a non-singular central point has ever been found. The singularity in the hollow-sphere-RCO center, i.e. in the center of its internal vacuum void, is the Big-Bang type singularity; everything is attracted away from the center. Hence, this singularity does not represent any problem. (If the Big-Bang type singularity was not acceptable, the theory of Big Bang would be incorrect.) Furthermore, this singularity is an abstract singularity, which exists in our description of the metrics in the vacuum void. In principle, no material particle can ever enter the singularity until it exists. The singularity is removed by an object with an energy comparable with the energy of the RCO, when this object occurs in the void.

In conclusion, we should seriously consider the concept of the hollow-sphere RCO with the outward oriented gravitational action and negative metric function  $u$  in its most central region. Although this concept includes a Big-Bang type, abstract singularity in the center, it is completely consistent with GR. In contrast to the hollow-sphere concept of RCO, the traditional, fulfilled-sphere concept requires the ignorance of GR in the RCO's central region.

We demonstrated that no predicted property of the hollow-sphere RCO contradicts the observations. On the contrary, it seems that such the concept can help us to solve several astrophysical and cosmological problems. The existence of the hollow-sphere RCO is predicted within the original GR, which is currently not the main-stream theory in the astrophysics of the compact objects, because of the postulated limitation. A discussion about the removal of the limitation is strongly desirable. Likely, we do not need any new physics. We should only use the whole extent of authentic, genuine, Einstein's theory of general relativity.

**Acknowledgements.** This work was supported, in part, by VEGA - the Slovak Grant Agency for Science, grant No. 2/0009/22.

## References

- Anastopoulos, C. & Savvidou, N., Classification theorem and properties of singular solutions to the Tolman-Oppenheimer-Volkoff equation. 2021, *Classical and Quantum Gravity*, **38**, 075024, DOI: 10.1088/1361-6382/abdf26
- Birkhoff, G. D. & Langer, R. E. 1923, *Relativity and modern physics* (Harvard University Press)
- Buchdahl, H. A., General-Relativistic Fluid Spheres. III. a Static Gaseous Model. 1967, *Astrophysical Journal*, **147**, 310, DOI: 10.1086/149001
- Chandrasekhar, S., The highly collapsed configurations of a stellar mass (Second paper). 1935, *Monthly Notices of the Royal Astronomical Society*, **95**, 207, DOI: 10.1093/mnras/95.3.207
- Chandrasekhar, S., The increasing role of general relativity in astronomy. 1972, *The Observatory*, **92**, 160
- deLyra, J. L., Energetic Stability of the Solutions of the Einstein Field Equations for Spherically Symmetric Liquid Shells. 2021, *arXiv e-prints*, arXiv:2101.07214, DOI: 10.48550/arXiv.2101.07214
- deLyra, J. L., The black-hole limits of the spherically symmetric and static relativistic polytrope solutions. 2023, *General Relativity and Gravitation*, submitted
- deLyra, J. L. & Carneiro, C. E. I., Complete solution of the Einstein field equations for a spherical distribution of polytropic matter. 2023, *General Relativity and Gravitation*, **55**, 67, DOI: 10.1007/s10714-023-03115-6
- deLyra, J. L., de A. Orselli, R., & Carneiro, C. E. I., Exact solution of the Einstein field equations for a spherical shell of fluid matter. 2023, *General Relativity and Gravitation*, **55**, 68, DOI: 10.1007/s10714-023-03116-5
- Einstein, A., Die Feldgleichungen der Gravitation. 1915, *Sitzungsberichte der Königlich Preussischen Akademie der Wissenschaften*, **XLVIII**, 844
- Einstein, A., Die Grundlage der allgemeinen Relativitätstheorie. 1916, *Annalen der Physik*, **354**, 769, DOI: 10.1002/andp.19163540702

- Hajj-Boutros, J., Radiation Equilibrium in General Relativity: General Solution. 1989, *Modern Physics Letters A*, **4**, 427, DOI: 10.1142/S0217732389000514
- Hansen, C. J. & Kawaler, S. D. 1994, *Stellar Interiors. Physical Principles, Structure, and Evolution*. (Springer)
- Hernández, H., Suárez-Urango, D., & Núñez, L. A., Acceptability conditions and relativistic barotropic equations of state. 2021, *European Physical Journal C*, **81**, 241, DOI: 10.1140/epjc/s10052-021-09044-5
- Ivanov, B. V., Analytical study of anisotropic compact star models. 2017, *European Physical Journal C*, **77**, 738, DOI: 10.1140/epjc/s10052-017-5322-7
- Kotopoulos, D. & Anastopoulos, C., Thermodynamics of spherically symmetric thin-shell spacetimes. 2023, *Classical and Quantum Gravity*, **40**, 225005, DOI: 10.1088/1361-6382/acfec1
- Misner, C. W., Thorne, K. S., & Wheeler, J. A. 2017, *Gravitation* (Princeton University Press)
- Murk, S., Nomen non est omen: why it is too soon to identify ultra-compact objects as black holes. 2022, *arXiv e-prints*, arXiv:2210.03750, DOI: 10.48550/arXiv.2210.03750
- Neslušan, L., The Ni's Solution for Neutron Star and Outward Oriented Gravitational Attraction in Its Interior. 2015, *Journal of Modern Physics*, **6**, 2164, DOI: 10.4236/jmp.2015.615220
- Neslušan, L., A solution to unconstrained Einstein's equations for a relativistic radiation sphere. in , *New Frontiers in Black Hole Astrophysics*, ed. A. Gomboc, Vol. **324** (Cambridge University Press), 355
- Neslušan, L., Outline of the concept of stable relativistic radiation sphere. A model of quasar? 2017b, *Astrophysics and Space Science*, **362**, 48, DOI: 10.1007/s10509-017-3027-x
- Neslušan, L., The second rise of general relativity in astrophysics. 2019, *Modern Physics Letters A*, **34**, 1950244, DOI: 10.1142/S0217732319502444
- Neslušan, L., A demonstration of the difference between the normalized and non-limited solutions of the field equations in the modeling of relativistic compact objects. 2022, in *Cosmology on Small Scales 2022*, ed. M. Krížek & Y. V. Dumin (Institute of Mathematics, Czech Academy of Sciences), 85
- Neslušan, L., Component  $x$  of the gravitational acceleration in general relativity and concept of mass. 2023, *Contributions of the Astronomical Observatory Skalnaté Pleso*, **53**, 16, DOI: 10.31577/caosp.2023.53.2.16
- Ni, J., Solutions without a maximum mass limit of the general relativistic field equations for neutron stars. 2011, *Science China Physics, Mechanics, and Astronomy*, **54**, 1304, DOI: 10.1007/s11433-011-4350-9
- Oppenheimer, J. R. & Snyder, H., On Continued Gravitational Contraction. 1939, *Physical Review*, **56**, 455, DOI: 10.1103/PhysRev.56.455
- Oppenheimer, J. R. & Volkoff, G. M., On Massive Neutron Cores. 1939, *Physical Review*, **55**, 374, DOI: 10.1103/PhysRev.55.374

- Penrose, R., Gravitational Collapse: the Role of General Relativity. 1969, *Nuovo Cimento Rivista Serie*, **1**, 252
- Schwarzschild, K., Über das Gravitationsfeld einer Kugel aus inkompressibler Flüssigkeit nach der Einsteinschen Theorie. 1916, in *Sitzungsberichte der Königlich Preussischen Akademie der Wissenschaften zu Berlin*, 424
- Stephani, H., Kramer, D., MacCallum, M., Hoenselaers, C., & Herlt, E. 2009, *Exact Solutions of Einstein's Field Equations* (Cambridge University Press)
- Straumann, N. 2013, *General Relativity* (Springer)
- Tolman, R. C. 1934, *Relativity, Thermodynamics, and Cosmology* (Clarendon Press)
- Tolman, R. C., Static Solutions of Einstein's Field Equations for Spheres of Fluid. 1939, *Physical Review*, **55**, 364, DOI: 10.1103/PhysRev.55.364
- Tolman, R. C. & Ehrenfest, P., Temperature Equilibrium in a Static Gravitational Field. 1930, *Physical Review*, **36**, 1791, DOI: 10.1103/PhysRev.36.1791
- Tooper, R. F., Adiabatic Fluid Spheres in General Relativity. 1965, *Astrophysical Journal*, **142**, 1541, DOI: 10.1086/148435
- Turck-Chieze, S., Cahen, S., Casse, M., & Doom, C., Revisiting the Standard Solar Model. 1988, *Astrophysical Journal*, **335**, 415, DOI: 10.1086/166936
- Whittaker, J. M., An Interior Solution in General Relativity. 1968, *Proceedings of the Royal Society of London Series A*, **306**, 1, DOI: 10.1098/rspa.1968.0133